Mechanisms of pattern formation from dried sessile drops

Mechanisms of Pattern Formation from Dried Sessile Drops

Maryam Parsa, [1,2] *Souad Harmand,* [1,2] *and Khellil Sefiane* [3,4]

[1]LAMIH Laboratory, CNRS UMR 8201, University of Valenciennes, Valenciennes 59313, France

[2]University of Lille Nord de France, Rue Jules Guesde, Villeneuve d'Ascq 59658, France

[3]School of Engineering, Kings Buildings, University of Edinburgh, Edinburgh EH9 3JL, United Kingdom

[4]International Institute for Carbon-Neutral Energy Research (I2CNER)

Kyushu University, 744 Motooka, Fukuoka 819-0395, Japan

Abstract

The formation of patterns after the evaporation of colloidal droplets deposited on a solid surface is an everyday natural phenomenon. During the past two decades, this topic has gained broader audience due to its numerous applications in biomedicine, nanotechnology, printing, coating, etc. This paper presents a detailed review of the experimental studies related to the formation of various deposition patterns from dried droplets of complex fluids (i.e., nanofluids, polymers). First, this review presents the fundamentals of sessile droplet evaporation including evaporation modes and internal flow fields. Then, the most observed dried patterns are presented and the mechanisms behind them are discussed. The review ends with the categorisation and exhaustive investigation of a wide range of factors affecting pattern formation.

Keywords

Sessile droplets; colloidal droplets; wetting; evaporation; pattern formation; desiccation patterns.

Contents

1. Introduction

It is known that having a solid-liquid-vapour system, such as a liquid drop deposited on a solid substrate, in equilibrium state is rare due to the sensitivity of fluids to variations in environmental conditions (i.e., pressure, temperature), which leads to the transition from one phase to another. Phase change is a process in which molecules of a certain phase (solid, liquid or vapour) lose or gain enough energy to shift into another phase. Evaporation is a type of phase change whereby liquid molecules near the air-liquid interface have sufficient energy to transit from a liquid phase to gas phase. This is conditional to the atmosphere around the drop surface should being not saturated with the vapour of the liquid.

Drop evaporation phenomenologically may seem a rather simple problem. However, from a purely scientific point of view, it is a complex problem, which is an important topic of interest to diverse scientific communities and for more than a century. The earliest investigation on the evaporation of micrometre-sized droplets was reported by Gudris and Kulikowa in 1924 [1]. Almost four decades later in 1962, Mangel and Baer [2] were the first to study the evaporation of sessile droplets on solid surfaces. The effect of various parameters on these volatile sessile droplets has been extensively explored, including ambient conditions, substrate properties and roughness. The evolution of droplet profile and dynamics of the contact line are dependent on these parameters. Apart from this, the nature and characteristics of the flow structure inside the evaporating droplets can be influenced by these parameters.

Another topic that has attracted great interest amongst researchers, over the last two decades, is the evaporation of sessile droplets containing insoluble particles. The pioneering

works of Deegan and co-workers [3–5] showed that particles can be moved towards the pinned contact line due to a convective outward flow and thus deposited at the droplet edge, forming a ring-like deposition pattern. This phenomenon is known as the "coffee-ring" effect. Following these pioneering publications, the evaporation of colloidal sessile droplets with the aim to control the morphology of deposition patterns left behind evaporation has been the subject of numerous studies for many scientific and industrial applications [6,7]. The studies on the drying of colloidal suspension droplets have revealed that there are different mechanisms behind the final particles distribution including the dynamics of the inner flow, evaporation kinetics, dynamics of the contact line, evolution of the droplet profile, interparticle and interfacial interactions. These mechanisms that may lead to the formation of particular deposition patterns, can be modified and controlled by manipulating a series of factors such as solute (i.e. size, concentration) [8,9], base fluid composition (i.e., surfactant) [10–13], environmental conditions (i.e., temperature, pressure) [14,15], etc. Therefore, understanding of the effects of the aforementioned factors is of paramount importance for both the control and reproducibility of the deposition patterns [6,7].

In addition to the aforementioned findings, another topic of interest is the evaporation of sessile droplets of complex fluids such as nanofluids, polymer suspensions, and biological fluids. The study of the dried patterns of biological fluids first begun in the former Soviet Union about three decades ago [16]. It was later found that the drying of the urine droplets of patients with urolithiasis would form a distinct pattern [17]. After these observations, the Ministry of Health of Russia developed the so-called "Litos" test system, which provides the preclinical diagnosis of urolithiasis [18]. In recent years, researchers have paid much attention to the pattern formation of biofluids (i.e., blood, tear, serum) which can be used as fast and cost-effective tools for diagnosis of some diseases [19–24]. The study of biofluid droplets is complicated as they consist of various components (i.e., electrolytes, proteins) which can

interact with each other and thus influence the underlying mechanisms involved in pattern formation [6]. Another type of complex fluids are polymer solutions which are non-Newtonian fluids, and mechanisms behind their evaporation are not well understood [6]. Polymers play an important role in the study of droplet evaporation as they are often added into the base fluids to modify the pattern formation for inkjet printing applications. A novel type of complex fluids are nanofluids which are the dispersion of metallic or non-metallic particles with at least one dimension in the nanoscale (< 100 nm) into a base fluid [25]. Since 1995, the studies on the evaporation of nanofluids has been rapidly increasing in number due to their wide applications in electronics cooling [26], boiling [27], solar energy [28], medicine [29], and automotive industry [30]. In spite of abundant number of studies devoted to applicability of nanofluids, the full understanding of mechanisms underpinning the drying of nanofluid droplets and their pattern formation still remains elusive.

It is well understood that the rapid increasing number of studies on the particulate deposition from droplets is due to the fast-growing demand for its applications in fields such as inkjet printing [31–33], paints, nanotechnology [34], and biomedicine [19,35,36]. Despite the importance of controlling deposition patterns and numerous dedicated studies, the mechanisms behind the deposition morphology of droplets are not yet fully understood [6]. Drying of even pure sessile droplets is a complex and difficult to control phenomenon, thus much research is needed on the drying of droplets of complex fluids.

This work presents a review of the experimental studies related to drying patterns from the evaporation of colloidal droplets. First, the evaporation modes and internal flow structure of sessile droplets are explained. Then, the most observed and important deposition patterns are introduced and discussed. Finally, the effects of most significant factors on pattern formation of particles are categorised and discussed. This review paper highlights the factors that are not extensively discussed in other review papers such as particle shape [37–39], mixing particles

with different materials and sizes [40], wettability of substrate [41–46], substrate temperature [13,15,44,47,48], manipulating base fluid composition (i.e., addition of alcohol) [11,13,49], etc. In addition, the most recent developments in the published studies related to the effect of various factors on pattern formation are reviewed, particularly for the past four years.

2. Sessile droplet evaporation

A sessile droplet is a liquid droplet which is placed on a solid substrate where its contact line limits the wetted contact area between the liquid and the solid surface and characterized by droplet height (H), radius (R), and contact angle (θ). The droplet evaporates if the atmosphere around the droplet's interface is not saturated with the vapour of the solvent. Evaporation of sessile droplets is an important topic of interest for many applications such as micro-electronic cooling [50], medical diagnostic techniques [19,35], nanotechnology [34], painting, and printing [31–33], etc. Thus, it has attracted the attention of researchers and has led to a rapid increase in the number of publications since the 1980s.

2.1. Evaporation modes

Evaporation of sessile droplets tend to show four modes and all are depicted in Figure 1. These four evaporation modes are [51]:

i. The constant contact radius (CCR) mode, where the contact line is pinned and the contact radius and the wetted contact area between the droplet and substrate remain constant, whereas the contact angle decreases with time (Figure 1a). There is a linear evolution of volume loss with time, revealing a constant evaporation rate for the CCR mode [52–54]. This mode is often seen with sessile droplets on rough substrates.

ii. The constant contact angle (CCA) mode, where the wetted contact area shrinks and the contact angle remains unchanged leading to a non-linear decrease of volume with time

(Figure 1b) [55,56]. Typically, on smooth hydrophobic substrates, droplet evaporation is in the CCA mode.

Commented [MP1]: Answer to comment 1 by Reviewer 1.

iii. The mixed mode, where the evaporation mode gradually changes into another mode (Figure 1c) and sometimes both the radius and contact angle decrease simultaneously [51,57]. One of the most reported behaviours is the transition from CCR to CCA (Figure 1c) [51].

iv. The "stick-slip" mode, where the droplet is in the CCR mode (corresponding to a "stick" phase), but the contact line suddenly slips/depins into a new position leading to a smaller contact radius when the contact angle reaches a threshold, minimum value (corresponding to a "slip" phase). Then, the droplet is again in the CCR mode ("stick" phase) until the next depinning occurs. This pinning/stick and depinning/slip of the contact line may occur for several times until the complete evaporation (Figure 1d). The "stick" phase lasts for longer time and accounts for the majority of the droplet lifetime, but the "slip" phase occurs rapidly. In 1995, Shanahan introduced a simple theory for the "stick-slip" evaporation mode [58]. According to Shanahan [58] and co-workers [14,59,60], when a sessile droplet is in a thermodynamic equilibrium, the free surface/interfacial energies of the system is at its minimum level. The decrease in the contact angle of the pinned droplet leads to the increase of this free energy above an energy barrier [14,60]. The pinning effect is also attributed to a potential energy barrier. When the excess free energy attains the energy barrier at a critical contact angle, the system has sufficient energy to overcome the energy barrier. Hence the contact line slips to a new equilibrium position to dissipate the excess free energy [14,60]. The droplet evaporation may proceed with the successive repetition of this cycle of the "stick" and "slip" phases.

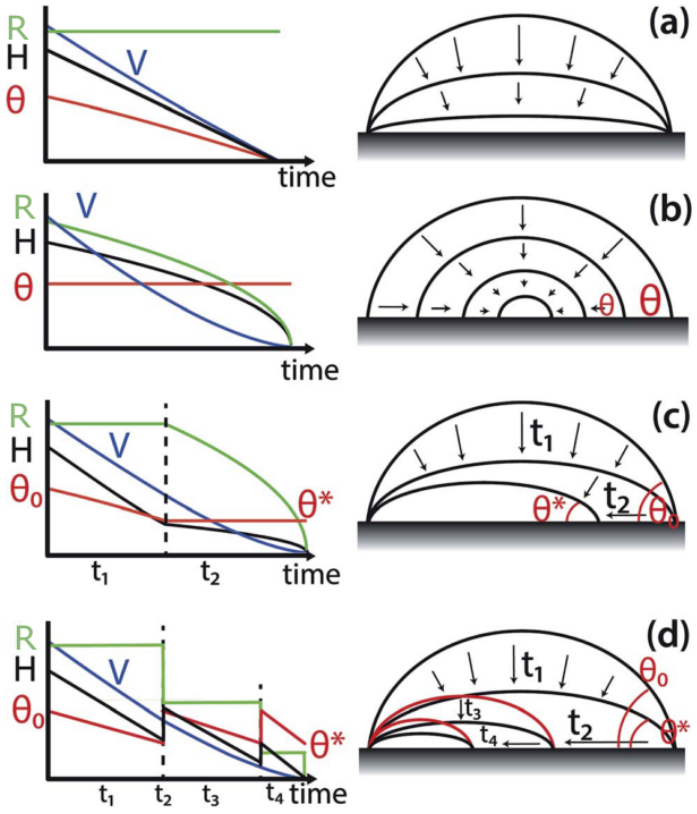

Figure 1. Schematic of the four possible evaporation modes of a sessile droplet: (a) Constant contact radius mode (CCR). (b) Constant contact angle mode (CCA). (c) Mixed mode (d) Stick-slip mode. The graphs show the evolution of the droplet profile (volume (V), height (H), contact radius (R), and contact angle θ) with time. Reprinted with permission from Ref. [51] Copyright (2015) Royal Society of Chemistry.

2.2. Flow fields within a drying droplet

The study of the effects of different flow fields within an evaporating sessile droplet is an important area in this research field. The capillary flow and Marangoni flow are two important flows which are commonly observed inside drying sessile droplets.

Once the contact line of a droplet is pinned on the solid surface, the fluid flows radially from the central region of the droplet towards the droplet edge due to the enhanced evaporation rate at the contact line. This radially outward flow replenishes the evaporated liquid at the edge, known as the capillary flow (Figure 2a) [3,61,62]. Within this particular flow field, the evaporating droplet usually follows CCR where the radius is constant and the contact angle decreases [6,7,63].

Marangoni flow is driven by the surface tension gradient along the free surface of the droplet [64]. This surface tension gradient is induced by the non-monotonous distribution of local temperature [64,65] and/or concentration along the liquid-vapour interface [10,61,64]. Usually, the flow is called the thermocapillary flow (or thermal Marangoni) in the case of the temperature gradient, and solutal Marangoni in the case of concentration gradient. In an evaporating droplet, the liquid tends to flow from lower surface tension regions towards higher surface tension regions, creating Marangoni convection (Figure 2b). Therefore, the direction of the Marangoni flow can change depending on how the surface tension is distributed along the interface. Kim et al. [66] showed that the direction of the Marangoni flow can be changed within a water droplet containing polymers by controlling the substrate temperature. In the case of heated substrates, the temperature at the edge is higher than that at the apex, and the evaporation is enhanced at the edge, leading to the non-uniformity of the evaporation rate along the interface. As the surface tension of water decreases with increasing temperature, the liquid flows from the edge towards the top of the droplet along the interface (Figure 3a) [66]. Conversely, cooling substrates generate the Marangoni flow in the opposite direction to that of heated substrates (Figure 3b) [66].

The cooccurrence of the capillary and Marangoni flows inside the droplets is possible when the solvent evaporation causes a thermodynamic and/or hydrodynamic instability [15,67]. Kim et al. [66] found that the capillary flow is stronger than the Marangoni flow when the substrate

is heated. In contrast, the Marangoni flow is more significant than the capillary flow in the case of cooled substrates.

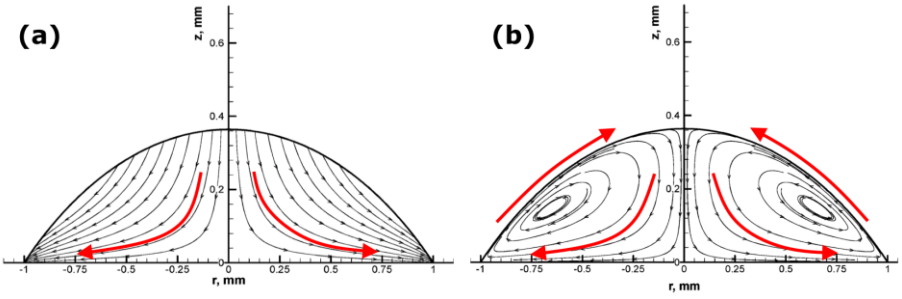

Figure 2. Streamline plots of the Flow field within a drying water droplet: (a) Capillary flow without Marangoni flow; Reprinted with permission from Ref. [62] Copyright (2005) American Chemical Society. (b) With Marangoni flow; The arrows indicate the direction of the flows. Reprinted with permission from Ref. [64] Copyright (2005) American Chemical Society.

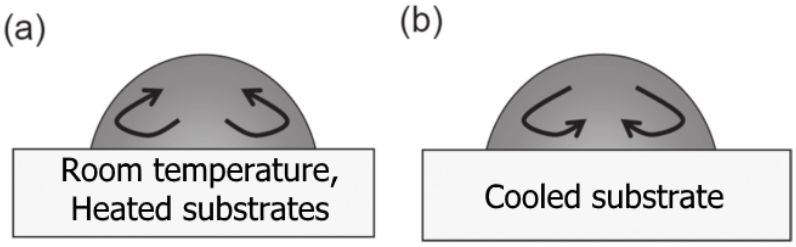

Figure 3. Schematic representation of the direction of the Marangoni flow inside drying water droplets: (a) Drying droplet at room temperature and heated substrate. (b) Drying droplet on cooled substrate. Reprinted with permission from Ref. [66] Copyright (2011) American Chemical Society.

3. Dried patterns formed by particles on the substrate

Drying liquid which contain non-volatile solutes is ubiquitous in daily life and nature such as stains after the drying of spilled tea/coffee drops on solid surfaces or rings of dust particles from dried rain drops on windows. The drying of sessile droplets with suspended particles forms various deposit patterns on solid surfaces. These interesting and complex patterns have significant influence in many applications such as biology [19,35,68], complex assembly [33], printing [31,69], nanotechnology [34], etc. Numerous studies have been published over the past decades to improve the understanding and controlling the deposition morphologies [6,7,63]. Macroscopic effects such as internal flow structure [4,70–72] and dynamics of the contact line [59,69,73,74], microscopic effects such as particle-interface/particle-particle interaction [75–77] significantly affect the morphologies of the final deposits. The most known of deposit patterns are described in the following subsections.

3.1. Coffee-ring pattern

When a droplet of coffee completely evaporates on a solid surface, it leaves behind a ring-like deposit of coffee, known as the coffee-ring pattern (see Figure 4). The related flow to this pattern is called the outward capillary flow. The geometrical constraint of the droplet behind the coffee-ring effect was explained in the pioneering work of Deegan and co-workers in 1997 [3]. They also studied the growth rate of the deposited ring, flow velocity and distribution of the particles inside the droplet [4]. During the formation of this pattern, the evaporating droplet is in the CCR mode, thus the droplet keeps its shape as a spherical cap. The height of the pinned droplet is decreased and hence the flow is pushed outward by the free surface. As the droplet is in the CCR mode and the radius is constant, liquid evaporated at the contact line must be replaced by liquid from the bulk (i.e. the centre of the drop). Thus, an outward flow inside the pinned droplet carries suspended particles towards the edge, leading to deposition of the particles near the contact line (Figure 5). After the complete evaporation, a ring of concentrated

particles can be seen at the perimeter of the droplet, forming the coffee-ring pattern (Figure 5) [3,24]. Uno et al. [78] studied the dried deposit of droplets on hydrophilic substrates. They found that thin layers of particle aggregates at the perimeter of the droplet were formed (Figure 6) and thus hindered the decrease of the wetted contact area (self-pinning). The rapid evaporation at the upper side of the layer induced the adsorption of particles to the substrate in the layer, forming the coffee-ring pattern. According to aforementioned explanations, there are two prerequisites for the formation of the coffee-ring effect: one is the droplet pinning (CCR); and the other is the higher evaporation rate at the pinned contact line than the rest of the droplet. Later, Hu and Larson [70] demonstrated that the only two conditions of the pinned contact line and continuous evaporation of liquid are not sufficient for having the coffee-ring pattern, but the suppression of a Marangoni flow is also required. The authors found that some particles deposit at the central region of the droplet due to a recirculating Marangoni flow induced by the surface tension gradient resulting from the evaporation [70]. Therefore, the Marangoni flow should be either reduced or eliminated by manipulating some parameters (i.e., substrate temperature) to create the coffee-ring pattern. Apart from the aforementioned conditions, the droplet size is also an important factor for creating the coffee-ring pattern [79]. Shen et al. [79] showed that a very rapid evaporation process inhibits a successful coffee-ring formation, as the suspended particles do not have sufficient time to reach and deposit at the edge. They experimentally demonstrated that there exists a lower limit of droplet size for having the coffee-ring pattern. For particle concentration above a critical value, the lower limit of the droplet size can be estimated by the competition between liquid evaporation and the diffusive particle motion inside the droplet. The minimum diameter of the droplet with the coffee-ring pattern was found to be approximately 10 nm for the particle size of 100 μm [79].

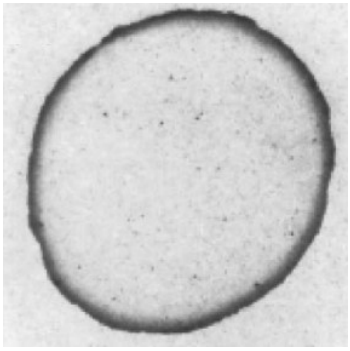

Figure 4. Coffee stain left after the drying of a coffee drop following the CCR mode. Reprinted with permission from Ref. [5] Copyright (2000) American Physical Society.

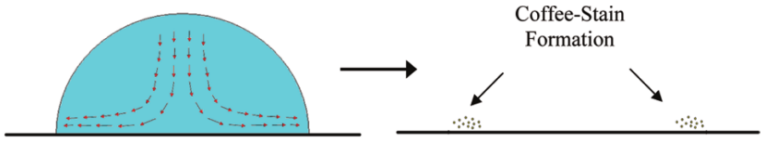

Figure 5. Evaporation of a colloidal drop under ambient conditions: Outward flow in a droplet creates a coffee-ring stain. Reprinted with permission from Ref. [71] Copyright (2012) American Chemical Society.

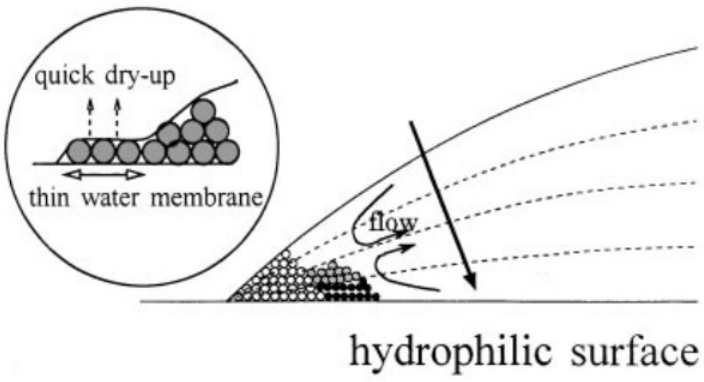

Figure 6. A schematic representation of particles motion and pattern formation inside a drying droplet on a hydrophilic surface with CCR mode. Inset shows the magnification of the contact line. Reprinted with permission from Ref. [78] Copyright (1998) Springer.

Commented [MP2]: Answer to comment 4 by Reviewer 2

3.2. Uniform pattern

Much attention has been devoted to altering the "coffee-ring" effect as uniform deposition patterns are required in many research fields such as coating [80], inkjet printing [69], and biological assays [81]. However, such uniform patterns are not easy to achieve due to the domination of the "coffee-ring" effect inside the droplet [81]. As mentioned in the previous section, the evaporation of droplets in CCR mode with the either sufficient suppressed or elimination of the Marangoni effect leads to the formation of the coffee-ring pattern. In the case of high concentration of particles, a drying droplet in CCR (with the negligible Marangoni effect) may leave a ring-like pattern, but with the uniform distribution of particles in the region enclosed by the ring [82,83]. As an example by Thokchom et al. [72], a monolayered, uniform nanoparticle structure was left behind after the dry-out of droplets on hydrophilic substrates, in which the Marangoni effect was completely suppressed and the outward capillary flow dominated in the flow field. The concentration of nanoparticles was slightly higher than the theoretical concentration for filling the wetted contact area, inhibiting the coffee-ring effect.

The alteration of the internal flow may also form uniform patterns. Majumder et al. [71] showed that the recirculating Marangoni flow within a droplet on a hydrophilic substrate prevents particles from accumulating at the pinned edge and transports them towards the top of the droplet along the air-liquid interface (see Figure 7a). The Marangoni flow keeps the particle concentration homogenized, inhibits coffee-ring pattern and forming a uniform pattern (Figure 7a).

Uniform patterns can be also formed by controlling the evaporation kinetics and/or interactions inside the droplet (i.e., particle-particle, particle-substrate, and particle-liquid interactions) [76,77,84]. Bigioni et al. [76] reported a highly uniform, long-range-ordered compact monolayer of nanocrystals created by enhancing the evaporation rate and also attractive particles interaction with the free interface of the droplet. Similarly, Li et al. [77] demonstrated that the sufficient enhancement of evaporation rate leads to the accumulation of particles at the air-liquid interface rather than at the edge, surpassing the coffee-ring effect (see Figure 7b). Those particles located at the interface deposit in the interior, and hence form a uniform deposition of particles in the interior with a thicker ring at the edge (Figure 7b). In the work by Bhardwaj et al. [75], the solution pH was varied to modify the particle-particle and particle-substrate interactions, which led to the alteration of the final deposit patterns. At low pH value, particles in the vicinity of the substrate were attracted to the substrate and formed a ring-like pattern with a uniform deposition of particles in the interior of the ring due to the attractive particle-substrate interaction (see Figure 7c). At intermediate pH value, the aggregation of particles was formed as the particle-substrate interaction was weaker than the particle-particle interaction. Aggregates randomly covered the entire initial wetted contact area. However, at high pH value, the ring-like pattern was formed with almost no particle in the interior of the ring due to the strong repulsive particle-substrate interaction.

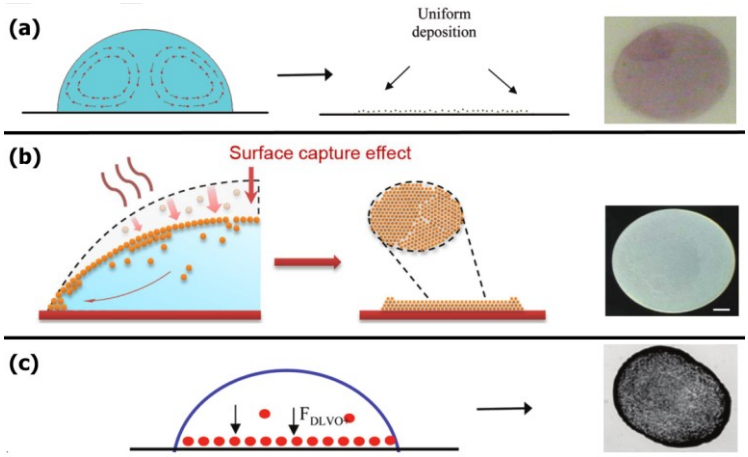

Figure 7. (a) Recirculating Marangoni flow creates a uniform pattern. Reprinted with permission from Ref. [71] Copyright (2012) American Chemical Society. (b) Rapid descending surface captures particles near the free interface, suppressing the coffee-ring effect and forming a uniform pattern. Reprinted with permission from Ref. [77] Copyright (2016) Nature Publishing Group. (c) Attractive forces between substrate and particles overcome outward flow and Marangoni convection, forming a uniform pattern with an outer thick ring. Reprinted with permission from Ref. [75] Copyright (2010) American Chemical Society.

Commented [MP3]: Answer to Comment 2 by Reviewer 1

3.3. Dot-like pattern

When a colloidal droplet follows the CCA mode while evaporating, a dot-like pattern can be found on the substrate after the complete evaporation, as shown in Figure 8 [72,85]. Uno et al. [78] studied the pattern formation of evaporating drops at CCA on hydrophobic surfaces. They reported that the shrinking of the contact line during the evaporation prevents particles from adsorbing onto the substrate at the early stages of the drying process. As evaporation proceeds, the concentration of particles increases which leads to the aggregation of particles. Then, the aggregates gather in the central region of the droplet and leaves a random pattern of tiny spots after the dry-out. Similarly, the other researchers observed such a dot-like pattern

left in the centre of dried droplets which followed the CCA mode (see Figure 8) [44,73,82]. Thokchom et al. [72] attributed the formation of such patterns on hydrophobic surfaces to the dominant inward Marangoni flow capable of transporting particles to the central region during the drying process. The Marangoni flow becomes weaker as the contact angle decreases with time, and a radially outward flow is generated close to the substrate at the late stages of the evaporation. However, the particle structures are already built within the droplet, and the outward flow is ineffective in transporting particles from centre to the edge. Therefore, the dot-like pattern is formed on the substrate after the dry-out (Figure 8). From the abovementioned studies, it can be deduced that the necessary condition to form the dot-like pattern is hydrophobic surfaces. The mechanisms behind this pattern formation on hydrophobic surfaces can be attributed to the CCA mode or/and the dominant inward Marangoni flow.

Commented [MP4]: Answer to Comment 3 by Reviewer 1

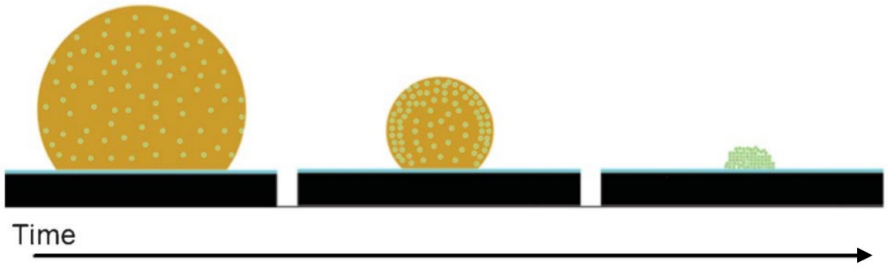

Figure 8. Evaporation of a droplet on a hydrophobic surface at CCA mode leads to the dot-like pattern. Reprinted with permission from Ref. [85] Copyright (2013) Royal Society of Chemistry.

3.4. Stick-slip pattern

If a colloidal droplet evaporates following the stick-slip mode, a set of concentric rings are left on the substrate after the complete evaporation [74], as shown in Figure 9a. During the "stick" phase of the "stick-slip" mode, particles accumulate at the contact line and form a ring. Then, the contact line slips to a new position, and particles again form another ring.

Consequently, the cycle of the "stick" and "slip" phases leads to the formation of a multiple concentric rings of particles on the substrate. The contact line usually sticks and slips on one side of the droplet, while it remains pinned on another side for all evaporation time, presumably due to the irregularities on the solid surface [82]. Unexpectedly, the study of the droplet profile showed that the sticking of the contact line is not complete during the "stick" phase; there is a slight drift of the contact line, known as the "pseudo-pinning" (see variation of the droplet radius over time in Figure 9b) [59,74,82,86]. Two explanations are proposed for the "pseudo-pinning" of the contact line: one is the small-scale pinning of the contact line by the deposited particles; and the other is the increased local viscosity at the contact line by the higher concentration of particles [59,74,86]. Adachi et al. [87] formulated a mathematical model to explain the mechanism behind the oscillatory motion of the contact line during the stick-slip mode, which leaves a striped pattern after the complete drying. The contact line bore a friction force when the particles move from the centre to the edge. The competition between the friction force and surface tensions at the contact line results in the oscillatory motion of the contact line, forming the striped stain pattern. Hence, the pinning or depinning of the contact line is not important because the competition between the forces determines the behaviour of the contact line [7,87].

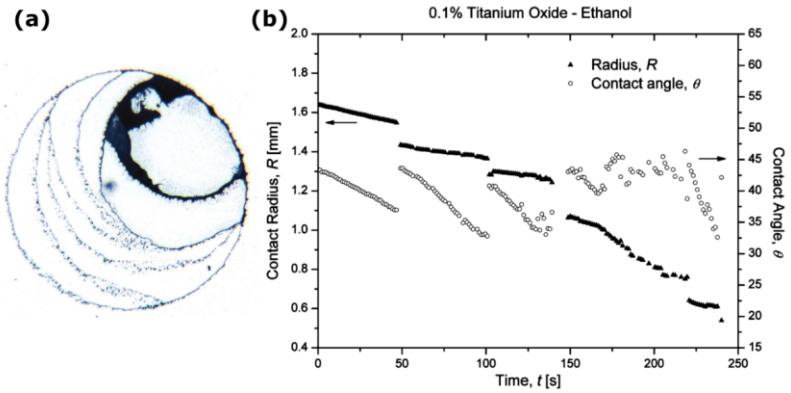

Figure 9. (a) "Stick-slip" pattern. Each ring of particles corresponds to the "stick" phase in the "stick-slip" mode. (b) Contact radius and contact angle versus evaporation time. Reprinted with permission from Ref. [74] Copyright (2009) American Chemical Society.

3.5. Fingering pattern

Apart from the aforementioned pattern types, a fingering pattern has been widely observed in many experiments of drop evaporation [88–91]. When a thin film or a droplet spreads on a substrate, a pattern can be formed with fingering structures along the edge of the spreading film or droplet. The competition between the capillary effects and the force causing the spreading can result in a hydrodynamic instability, and consequently led to the fingering phenomenon [92]. It is proved that the fingering instability is affected by the flow structures induced by temperature gradients [93], centrifugal forces [94], or gravity [95]. Weon and Je [96] observed the fingering pattern inside the peripheral ring after the evaporation of a bidispersed colloidal drop, as shown in Figure 10. The formation of the pattern was attributed to the competition between the outward capillary flow and the inward Marangoni flow. Crivoi and Duan [91] reported the formation of both symmetrical and asymmetrical fingering patterns after the full drying of CuO water-based nanofluid droplets. It was explained that the formation of the asymmetrical pattern can be due to the non-uniform evaporation rate or the movement of the contact line. Unexpectedly, a pinned droplet containing high concentrations of surfactants showed an outward fingering instability along the contact line [92]. The fluid was pushed outward in the fingering instability by local vortex cells arisen from both thermocapillary effects and the surfactant-induced Marangoni flow. As a result of this behaviour, the contact line deformed and a finger protruded from the evaporating water droplet, led to the collection of particles in the fingers of the droplet, as shown in Figure 11.

Commented [MP5]: Answer to Comment 9 by Reviewer 1

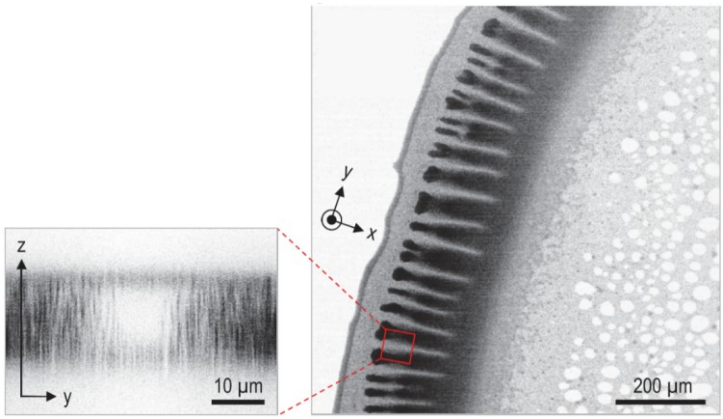

Figure 10. Fingering patterns inside the peripheral ring. Reprinted with permission from Ref. [96] Copyright (2013) American Physical Society.

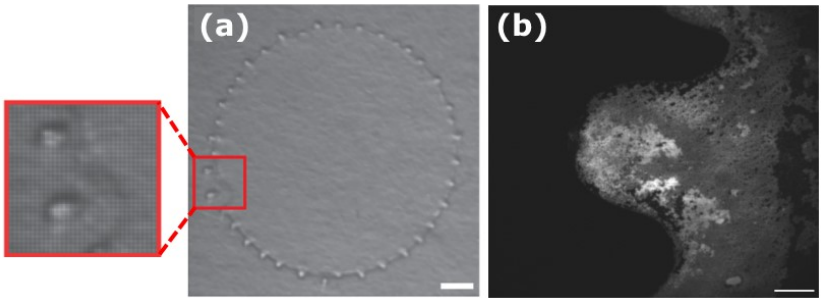

Figure 11. (a) Evaporating droplet fingering outward. (b) Particles in the fingers of the droplet. Reprinted with permission from Ref. [92] Copyright (2014) American Chemical Society.

3.6. Crack pattern

The investigation of cracking arising from desiccation of complex fluids is growing amongst scientific communities [20,22,24,36,63,97–101]. Varying suspension salinity led to the formation of crack patterns with different morphologies after drying a colloidal drop on a flat surface (see Figure 12) [97]. At low salinities (Figure 12a), radial cracks were regularly formed at the drop edge, while a disordered crack pattern formed at intermediate salinities

(Figure 12b,c). At large salt contents (Figure 12d), a unique circular crack pattern was left after evaporation. These behaviours were explained by the drop shape evolution (Figures 12aI-dI). For intermediate salt content, the observed disordered crack pattern was related to the formation of a solid gelled skin (Figure 12bII), and also to the following buckling instability. Overall, the shape evolution of the drop affects the number and direction of the cracks [19]. The evolution of the drop shape depends on the salt content, thus the morphology of crack patterns are different for various salt contents [19,97]. Furthermore, Crack patterns can be formed after drying of drops containing biological materials and fluids [20,22,24,36,39,98,101,102]. The higher evaporation rate at the edge of a droplet of blood plasma redistributes the suspended substances [63]. The accumulation of these substances at the edge region leads to the formation of a film (starting from the edge) which induces the gelation of the drying droplet. First, the drying starts from the edge, whereas the central region remains wet [103]. The evaporation induces the shrinkage of the droplet from the gelled edge which causes a local stress. However, the adhesion of the droplet to the substrate constrains this shrinkage-induced local stress. As a result, an increased tensile stress in a drying drop is created by the competition between the adhesion to the substrate and the shrinkage [97,98]. Once the local tensile strength is exceeded by the increased tensile stress, cracks are formed on the surface of the film [63].

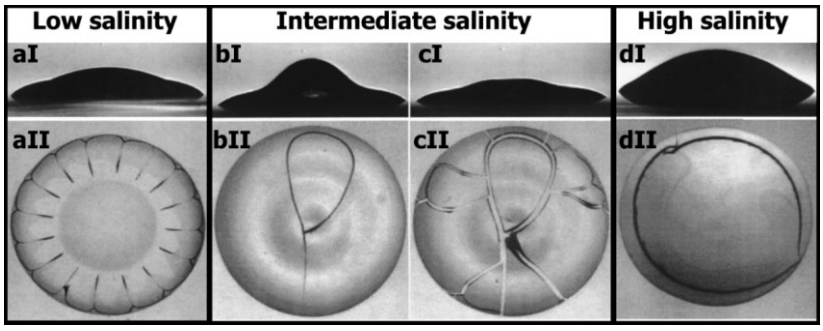

Figure 12. Influence of salt content on crack patterns from drying colloidal drops: (a) A regular radial crack pattern at low salinity. (b,c) A disordered crack pattern at intermediate salinity. (d) A circular crack pattern at high salinity. Side view of drops taken at: (aI) 15 min after deposition, (bI) 15 min after deposition, (cI) 20 min after deposition, and (dI) 15 min after deposition. Top view of drops taken at: (aII) 20 min after deposition, (bII) 20 min after deposition, (cII) 22 min after deposition, and (dII) 21 min after deposition. Reprinted with permission from Ref. [97] Copyright (1999) American Physical Society.

3.7. Crystal pattern

Crystallisation is often observed in the central regions of the dried droplets containing salts [104–106] (see Figure 13). The effect of different substrates and salt contents on crystal patterns from pure saline droplets are shown in Figure 13a [46]. The crystal patterns are fairly similar for the silicon and polymethyl methacrylate (PMMA) substrates, as shown in Figure 13aI,II. Regardless of the salt contents, the patterns are comprised of either a single cube or accumulated crystals in the centre of the dried droplets. The size of these crystals becomes larger with increasing the salt content. On the other hand, on the glass substrate, there is a cracked thin layer of crystal covering the initial contact area between the substrate and droplet (Figure 13aIII). Some isolated crystal cubes are also formed inside the dried droplets. On the silicon and PMMA surfaces with low wettability, the unique evaporative dynamics were

observed during which the contact angle increased in the middle of the evaporation and lasted for a long period. The long depinning stage was found as the main mechanism behind the formation of the crystal cube in the droplet centre. On the contrary, on the glass substrate with high wettability, the long pinning effect (or the CCR mode) was enough to overcome the depinning effect induced by the concentrating solution.

Apart from the pure saline solution, crystal patterns are also formed in saline solutions containing other compositions. The addition of polymer into the saline solutions promoted the pinning effect and prevented the formation of single square-shaped crystals in the centre of the dried droplets on a substrate with low wettability [106]. Therefore, the droplets containing the mixture of polymer and salt experienced the CCR mode until the salt crystallisation occurred. At high salt contents (Figure 13bVII-IX), the salt crystals formed near the periphery and formed a ring-shaped pattern. At intermediate salt content with a high polymer concentration (Figure 13bIV), a dendritic structure was formed inside the peripheral ring. However, at intermediate salt contents with lower polymer concentrations (Figure 13bV,VI), concentric rings were formed with a set of needle-shaped crystal structures at the centre. Fast evaporation near the contact line brought the liquid and solute toward the contact line. There were regions near the contact line where the local concentration was lower than the critical value, and on the other hand, there were regions at some distances away where the local concentration was higher than the critical value. The crystallisation occurred and a crystal ring was formed when the local concentration of the solute exceeds the critical value. Therefore, based on this mechanism, concentric rings were formed and the spacing between the rings was found to be proportional to the original salt contents in the mixture and the base radius. At low salt contents (Figure 13bI-III), no big crystals were observed and instead, a more uniform pattern were formed due to very low salt concentration.

Commented [MP6]: Answer to Comment 4 by Reviewer 1

For biological fluids containing salts, the combination of two evaporation modes of CCR and CCA during drying drops contributes to the formation of salt crystallisation in the interior regions of a thick peripheral ring [19,107]. As an example, Gorr et al. [19] studied pattern formation from drying drops of aqueous lysozyme protein solutions with different salt concentrations. They reported that the early separation of protein from the fluid promoted an outward capillary flow during the CCR mode and hence formed the thick outer ring by the protein (Figure 13cI). As evaporation proceeded, the contact angle decreased to a critical value and at that point, the salt crystallisation occurred while the drop depinned and receded toward the central regions. Thus, a grainy texture was formed in the centre of the dried drop (see inset in Figure 13cI). For higher salt concentrations, the formation of the outer ring was the same as the low salt solution (Figures 13cII-IV), but the droplet did not depin, leading to an increase in the capillary flow rate. Aggregates were formed and moved toward the contact line creating a secondary ring very close to the outer ring. Dendritic crystal structures were formed rapidly in the central regions in the late stages of the evaporation (see insets in Figures 13cII-IV). Increase in salt contents led to more dendrites in the centre of the dried droplets (see insets in Figures 13cII-IV). Some studies reported that inorganic salts and the aggregation of macromolecular proteins are the main contributors to the formation of crystal patterns in the centre [107–109]. It has been reported that the increase of inorganic salt contents augments the aggregation of macromolecular proteins and hence affects the final morphology of crystal patterns [63,97,105]. However, another explanation for the formation of crystal patterns is that these patterns are the salt crystals in the gelled protein matrix, and proteins only have the role of seeds for the salt crystal growth [63,110,111]. The underlying mechanisms behind crystal patterns are not fully understood as there are difficulties to distinguish the main components of these patterns by current analytical techniques [63].

Commented [MP7]: Answer to Comment 4 by Reviewer 1

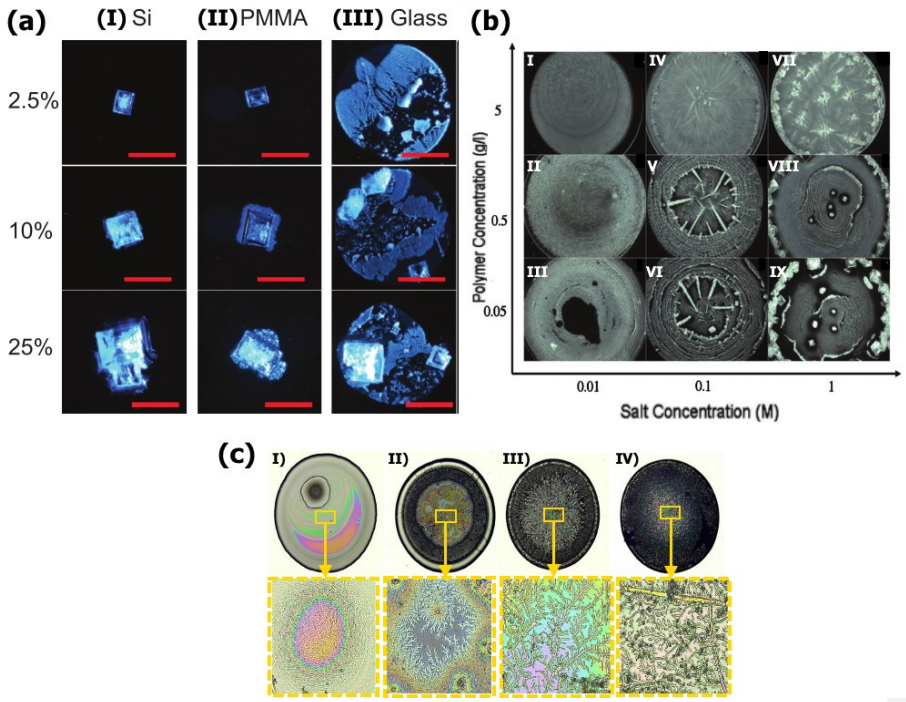

Figure 13. (a) Dried patterns from pure saline droplets with varying salt concentrations on different substrates: (I) hydrophobic silicon, (II) hydrophobic PMMA, and (III) hydrophilic glass. Scale bar, 1 mm. Reprinted with permission from Ref. [46] Copyright (2017) American Chemical Society. (b) Dried patterns from saline droplets containing polymer at different concentrations on a hydrophobic glass. Reprinted with permission from Ref. [106] Copyright (2010) American Institute of Physics. (c) Dried patterns from droplets of lysozyme solutions with varying salt concentrations: (I) 0.01 wt %, (II) 0.1 wt %, (III) 0.5 wt %, and (IV) 1 wt %. Reprinted with permission from Ref. [19] Copyright (2013) Elsevier.

Commented [MP8]: Answer to Comment 4 by Reviewer 1

3.8. Combined pattern

In some cases, a combined pattern of two or more pattern types appears on a substrate. As an example, Crivoi and Duan [112] reported the formation of the fingering pattern in the interior of the coffee-ring after the complete evaporation of a water-based copper nanofluid

droplet (Figure 14a). It was found that the nucleation and growth process inside the peripheral ring results in the formation of this combined pattern. A combined pattern of ring-like and dot-like patterns was observed after the full evaporation of a drop containing a mixture of surface-inactive and surface-active solutes on a substrate with weak contact angle hysteresis, as shown in Figure 14b [42]. By analysing the drop shape evolution during the last stage of the evaporation, it was found that the contact line was pinned due to surfactant adsorption and this led to the ring-like pattern formation. Then, the depinning of the contact line started from a corner, and most parts of the contact line receded towards the part that was unpinned. Finally, the precipitation of surface-inactive solutes occurred close to the pinned part of the contact line, and led to the dot-like pattern formation inside the peripheral ring. Nguyen et al. [113] observed inner coffee-ring deposits (ICRDs) inside the initially pinned contact area of the dried water-based SiO_2 nanofluid droplets on smooth hydrophobic substrates (Figure 14c). In addition, dendrite-shaped patterns were observed inside ICRDs. The formation of the combined patterns was explained by the late secondary pinning of the contact lines which occurred after the initial pinning. The balance of the forces on nanoparticles led to the secondary pinning. The size and patterns of ICRDs were found highly dependent on nanoparticle concentration, contact angle hysteresis, and nanoparticle interaction forces. Drying biofluid drops often form complex patterns which are the combination of different deposition patterns. Figure 14d shows the dried pattern of blood serum from a healthy person which is the combination of two crack and crystal patterns [114]. As shown in Figure 14d, the deposit is characterized by two parts: one is the peripheral part which is composed of radial and orthoradial cracks (Figure 14dI); the other is the central part which is composed of different morphologies of crystal pattern such as dendrites and inclusions (Figures 14dII,III).

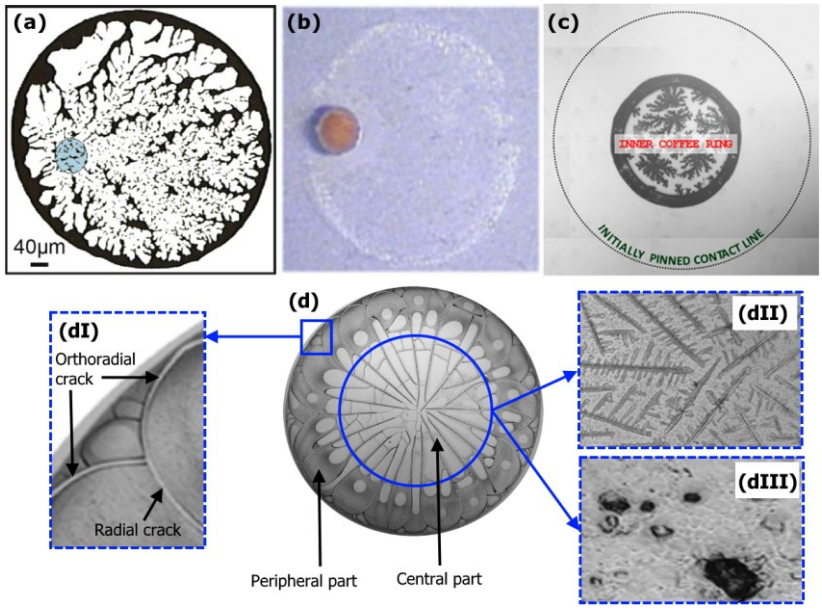

Figure 14. Combined patterns: (a) Fingering pattern inside the coffee-ring pattern. Reprinted with permission from Ref. [112] Copyright (2013) Elsevier. (b) Dot-like pattern inside the coffee-ring pattern. Reprinted with permission from Ref. [42] Copyright (2013) American Chemical Society. (c) Dendrite-shaped pattern inside the inner coffee-ring deposit. Reprinted with permission from Ref. [113] Copyright (2013) American Chemical Society. (d) Crystal pattern enclosed with the crack pattern: (I) Radial and orthoradial cracks in the peripheral part of the deposit, (II) Dendrites in the central part of the deposit, and (III) Inclusions in the central part of the deposit. Reprinted with permission from Ref. [114] Copyright (2014) Springer.

4. Effects of different factors on deposit patterns

In the previous section, a series of dried patterns are discussed which are significantly affected by evaporation kinetics, the movement of contact line, inner flow structure, interfacial interactions, and particle-particle interaction. The mentioned effects are dependent on the

Commented [MP9]: Answer to Comment 9c by Reviewer 1

factors which can be manipulated to control the pattern formation of drying drops. These factors that affect dried patterns are discussed in the next subsections.

4.1. Solute effect

Solute plays a significant role in the formation of deposition patterns. The effects of concentration, size, shape and material of solutes have been studied on the dried patterns. The influence of particle concentration on the final deposition patterns is still controversial in the literature. Some studies reported a transition from a coffee-ring pattern into a different pattern (i.e., uniform pattern) by increasing the concentration [9,45]. However, some do not report any changes in the coffee-ring pattern except that the thickness of the ring increased with concentration [36]. On the other hand, some studies have shown that the increase in the concentration led to the stick-slip behaviour [86]. It is noteworthy to mention that the size and material of particles are not identical in the relevant studies and these may affect the final deposition patterns.

Only few studies have done on the effect of particle shape on the final deposition patterns. These studies have shown that the change in the aspect ratio of particles led to the deterioration of the coffee-ring pattern in the case of hydrophobic particles [37]. In the case of hydrophilic particles, the aspect ratio had no effect on the patterns [38].

The results from the effect of particle size on the dried patterns are different, probably due to different particle concentration in these studies. Despite this, the majority of the studies have reported that smaller particles are more likely to form a coffee-ring pattern [115,116]. In the case of larger particles, they tend to mainly deposit in the central regions of the dried droplets [115,116].

Similar to the particle shape, the effect of particle material has not been studied well and hence, the number of studies in the literature is limited. One study shows that the change in

particle materials does not change the dried pattern significantly [45]. On the other hand, the other study shows that different particle materials form completely different patterns [40]. This discrepancy in the results may arise from different particle size and concentration in these studies. In the next subsections, the effect of solute on the deposition patterns has been extensively reviewed in terms of concentration, shape, size, and material.

Commented [MP10]: Answer to Comment 5 by Reviewer 1 and Answer to Comment 1 by Reviewer 2

4.1.1. Concentration

Particle concentration has a significant influence on the final deposition patterns. Sefiane [36] investigated the effect of concentration (0.1, 0.5, 1 and 2%) on the final deposition patterns of Al_2O_3 nanofluid drops. Ring-like patterns were observed for all concentrations and the thickness of the ring increased with increasing concentration. Cellular cracking patterns were also found which were more prominent at higher concentrations. Increasing concentration increased the thickness of these cells. Brutin [9] observed a transition between two patterns that corresponded to a critical concentration, as seen in Figure 15. For concentrations between 0.01 and 0.47 wt %, a coffee-ring pattern with no particles in the interior of the ring was formed. The width of the ring decreased with increasing concentration following a power law. For concentrations above 1.15 wt %, nanoparticles deposited in the central regions, forming a "flower petal" pattern. The deposition thickness increased with increasing concentration, whereas the number of "flower petals" decreased with concentration. As shown in Figure 16, a dot-like pattern was observed at polymer concentration of 0.5 wt %, while a ring-like pattern was observed at 3 wt % [117]. Lee et al. [45] showed that there is a transition from a coffee ring pattern to a uniform pattern with increasing concentration at the nanoparticle size of 135 nm. However, there was no obvious relation between concentration and the type of deposit patterns at lower nanoparticle sizes. Therefore, the authors combined the effects of both concentration and nanoparticle sizes. Low nanoparticle concentrations and small nanoparticle sizes formed a coffee-ring pattern, while high concentrations and large particle sizes led to the

formation of a uniform pattern. At moderate concentrations and particle sizes, an irregular pattern was formed. Moffat et al. [86] showed that drying nanofluid droplets with concentration of 0.01 wt % had a receding contact line with distinct decrease in contact angle. However, drying nanofluid droplets with concentration of 0.1 wt % showed the "stick-slip" behaviour. The increase of nanoparticle concentration enhances the "stick-slip" behaviour [59,86]. A direct correlation was found between the distance jump by the contact line and nanoparticle concentration [59]. The higher concentration leads to a longer pinning of the contact line, thus the deviation in contact radius from equilibrium before a jump is higher and the steps of the contact line are greater [59].

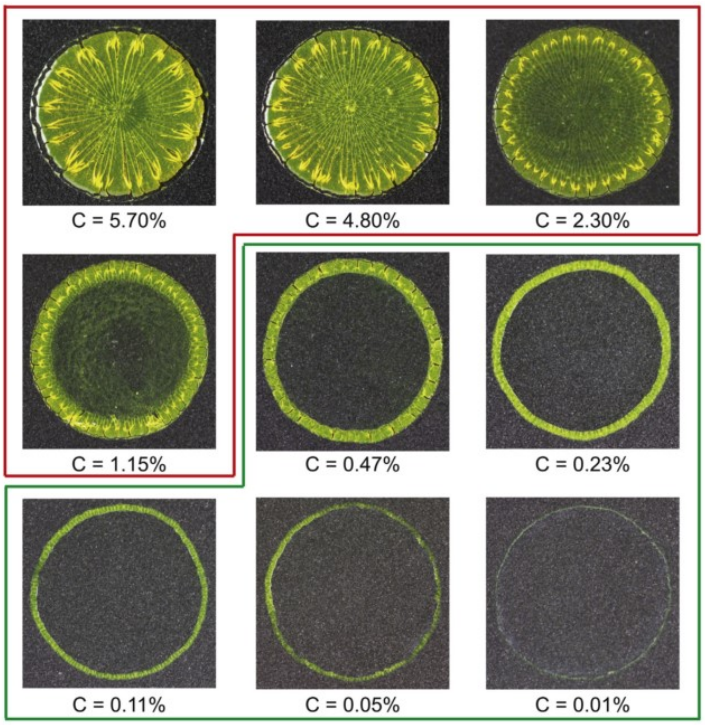

Figure 15. Influence of nanoparticle concentration on final deposition patterns. Coffee-ring pattern is formed for concentration between 0.11 and 0.47 wt %, and a flower petal pattern is

formed for concentration between 1.15 and 5.7 wt %. Reprinted with permission from Ref. [9] Copyright (2013) Elsevier.

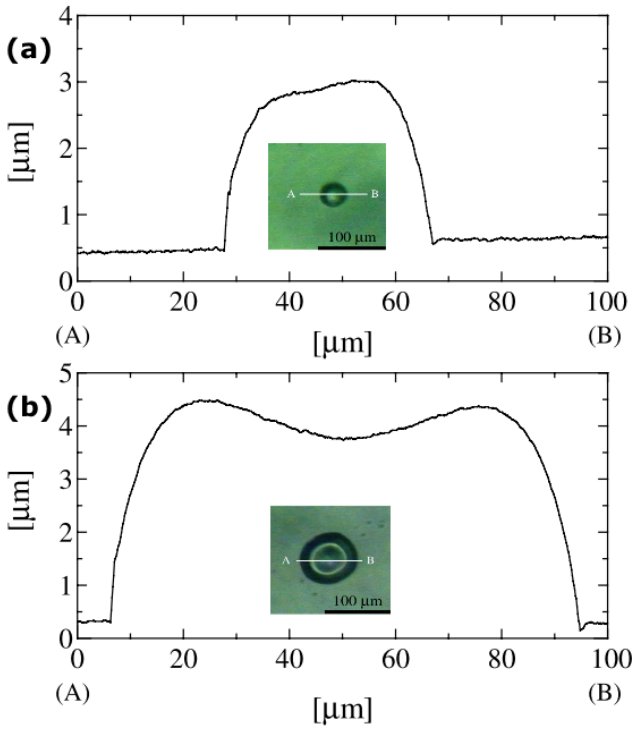

Figure 16. Dried patterns and thickness of polymer films: (a) A Dot-like pattern at concentration of 0.5 wt %. (b) A ring-like pattern at concentration of 3 wt %. Reprinted with permission from Ref. [117] Copyright (2006) Elsevier.

4.1.2. Shape

Interfaces are significantly deformed by the anisotropic shape of particles, generating strong particle-particle interactions [118–124]. The outward flow which is responsible for the generation of the coffee-ring effect for spherical particles, carries ellipsoidal particles to the air-liquid interface causing strong long-ranged particle-particle attractions amongst ellipsoidal particles. Consequently, loosely packed aggregates are formed at the air-liquid interface

[118,119,123,125]. Similarly, Yunker et al. [37] demonstrated that the addition of ellipsoidal particles to suspensions containing spherical particles can deteriorate the coffee-ring effect. They found that the coffee-ring persisted if the minor axis of ellipsoidal particles is larger than the diameter of spherical particles; the coffee-ring is inhibited if the axis is smaller than the diameter. Thus, in the presence of ellipsoidal particles with appropriate aspect ratio, a loosely-packed structure can be formed at the free surface of evaporating drops, preventing particles from reaching the contact line and resulting in a uniform pattern after dry-out (Figure 17a). However, in the absence of ellipsoidal particles, the drying of drops containing spherical particles forms the coffee-ring pattern (Figure 17b). Dugyala and Basavaraj [38] studied the effect of both particle shape and the pH of the solution containing hematite ellipsoids. As shown in Figure 18, there is no considerable change in the deposit patterns for different particle aspect ratios at each pH value, while the type of the deposit patterns is changed for different pH values at each aspect ratio. The coffee-ring pattern is formed for low and high pH values, and the uniform pattern is formed for intermediate pH values. It is noteworthy that the particles in their study were hydrophilic, while the particles used in the study of Yunker et al. [37] were partially hydrophobic. A transition was found from radial to circular crack patterns by changing the particle shapes from spheres to ellipsoids [39]. The different aspect ratios of ellipsoidal particles had no significant effect on the crack patterns, and the same circular crack patterns were produced. It was found that the crack patterns formed by anisotropic particles are significantly affected by the particle ordering rather than their aspect ratio.

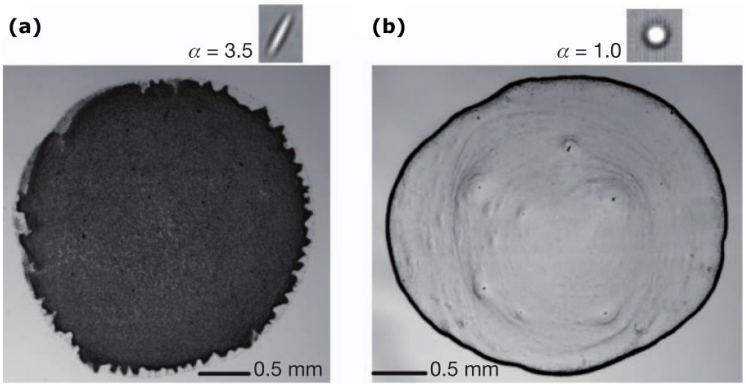

Figure 17. (a) Uniform pattern formed by ellipsoidal particles. (b) Coffee-ring pattern formed by spherical particles. α is major-minor axis ratio. Reprinted with permission from Ref. [37] Copyright (2011) Nature Publishing Group.

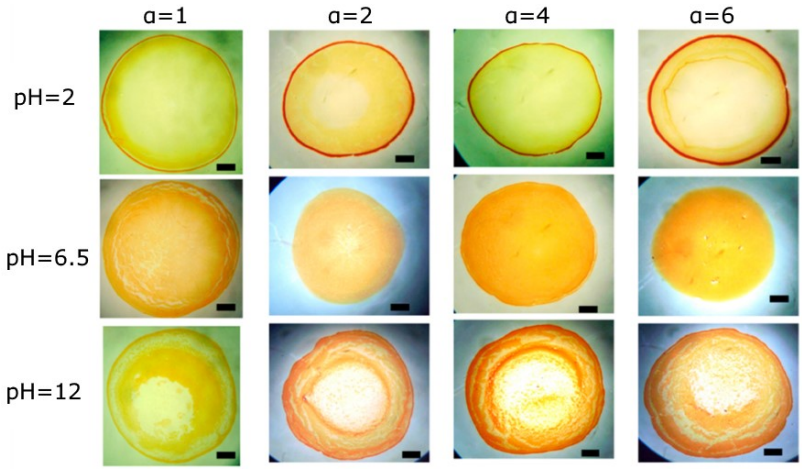

Figure 18. Effect of hematite particle aspect ratio (α) and pH of solution on final deposit patterns. Reprinted with permission from Ref. [38] Copyright (2014) American Chemical Society.

4.1.3. Size

Chon et al. [8] studied the influence of the different sizes of nanoparticles (2, 11, 30, and 47 nm) on the pattern formation. Larger nanoparticles led to the formation of the distinctive coffee-ring patterns, but smaller nanoparticles formed a thicker and more uniform deposition in the central region enclosed with a loosely defined wider ring. A different work by Choi et al. [115] investigated the pattern formation from evaporating water drops containing polystyrene particles (1 and 6 μm) and hollow glass spheres (9-13 μm). For the large-sized polystyrene particles, the contact line was not pinned and receded during the evaporation. Some particles deposited at the edge, but the considerable number of particles deposited in the interior region of the ring. The small-sized polystyrene particles moved towards the pinned edge and formed the coffee-ring pattern. In the case of hollow glass particles with a mix of small and large sizes, the contact line was not pinned and particles moved inward along the air-liquid interface and finally deposited in the centre of the droplet at the final stages of evaporation. A phase diagram in terms of polymer concentration and poly(methyl methacrylate) (PMMA) colloid size was obtained by Ryu et al. [116]. As demonstrated in Figure 19, in the absence of polymer, small colloids form the coffee-ring pattern, while larger colloids are randomly distributed in the droplet forming bump-like patterns. At low polymer concentration of 0.1 wt %, the coffee-ring effect is enhanced by increasing colloid size from 0.1 to 1 μm. The same trend is observed with increasing size from 5 to 10 μm, but the coffee-ring effect is more pronounced for the colloid size of 1 μm than larger colloids. At each of high polymer concentrations (0.5 and 1 wt %), the coffee-ring effect is enhanced with increasing colloid size, and large colloids form the coffee-ring patterns. The aggregation dynamics of colloids depends on their size. In the presence of polymer, small colloids are likely to build aggregation than large ones, implying that the interactions between colloid and polymer for large-sized colloids become weak and thus the coffee-ring effect becomes dominant.

There are also studies wherein the effect of particles with multiple sizes in a single liquid drop on the final deposit was investigated. As an example, Sommer et al. [126] studied the effect of two different particle sizes (60 and 200 nm) in a liquid drop on the distribution of particles on a smooth substrate. The slow evaporation of drops resulted in well-ordered structures, where larger particles formed a peripheral ring in dense hexagonal structures, surrounding the massive inner ring. However, the study by Jung et al. [127] showed the mixture of multi-sized particles (500 nm and 5 μm) led to a different deposition pattern. During the evaporation process, nanoparticles moved towards the contact line and enhanced the pinning effect, while microparticles moved towards the centre of the droplet resulting from the surface tension force of the liquid. As a result of this particles motion, larger and smaller particles separately deposited onto the substrate. Larger particles accumulated in the centre of the dried drop enclosed with a ring formed by smaller particles. Similarly, a separation of particles with three different sizes in a liquid droplet was reported (Figure 20) [128]. Three well-separated rings were formed near the contact line by each size. The outermost ring was formed by the smallest particles, while the innermost ring was built by the largest particles. This concept of particle separation based on the particle-size effect can be a natural, cost effective method for disease diagnostics. The schematic phase diagram in Figure 21 shows the effect of particle volume fractions of small and large particles on the final pattern after evaporation of a decalin-based colloidal droplet [96]. Coffee-ring patterns were formed for monodispersed small colloids, and increased with increasing the concentration of the small colloids. For monodispersed large colloids, bump-like patterns were formed and increased with increasing the concentration of the large colloids. For bidispersed colloids at lower concentration, fingering patterns were left after the complete evaporation due to the competition between the outward coffee-ring and inward Marangoni effects, particularly when the Marangoni flow was suppressed by the coffee-ring flow. The formation of multiple ring patterns for bidispersed

colloids was attributed to the particle separation based on the size. For high concentrations of bidispersed colloids, a pronounced ring-like pattern was left behind. Recently, Zhong et al. [40] carried out experiments to study the effect of multi-sized particles on pattern formation. As shown in Figure 22, the non-uniform deposition patterns left either by 5 or 40 nm Al_2O_3 nanoparticles. For the weight ratio from 0:1 to 2:8 (Figure 22a), the droplet shrinkage occurred in the middle of the evaporation, while those droplets with the weight ratio above 2:8 were pinned until the late stages of the evaporation (Figure 22b), preventing the large nanoparticles from making aggregates at the contact line and thus the formation of the fractal-like structures. By further increase of the 5 nm nanoparticles from the weight fraction of 30 to 50% (Figure 22b), the attraction between the small and large nanoparticles suppressed the movement of the small ones towards the central region. Therefore, the non-uniformity of the patterns left either by pure 5 or 40 nm nanoparticles was eliminated by combining of the proper concentration of the two nanoparticle sizes.

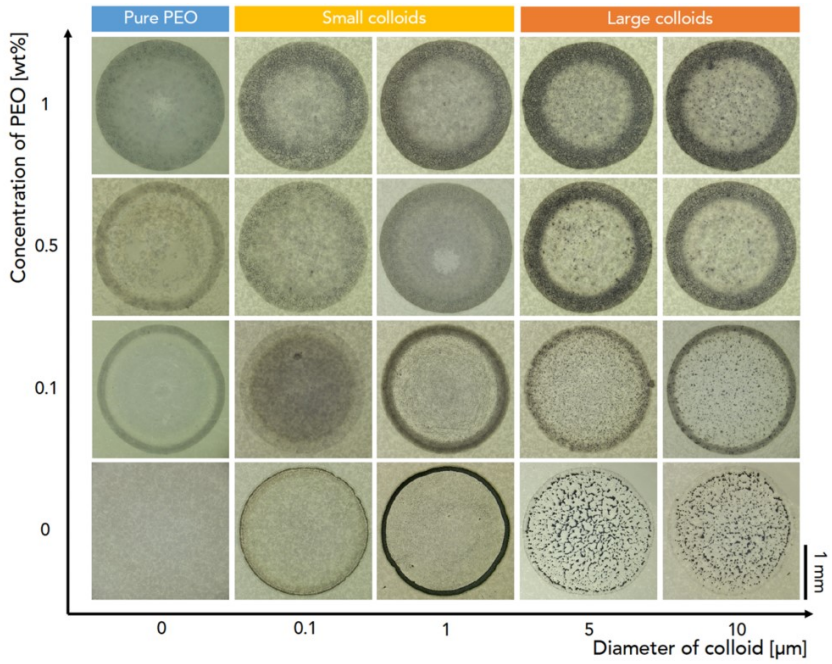

Figure 19. A phase diagram for polymer concentration and poly(methyl methacrylate) (PMMA) colloid size. Reprinted with permission from Ref. [116] Copyright (2017) Nature Publishing Group.

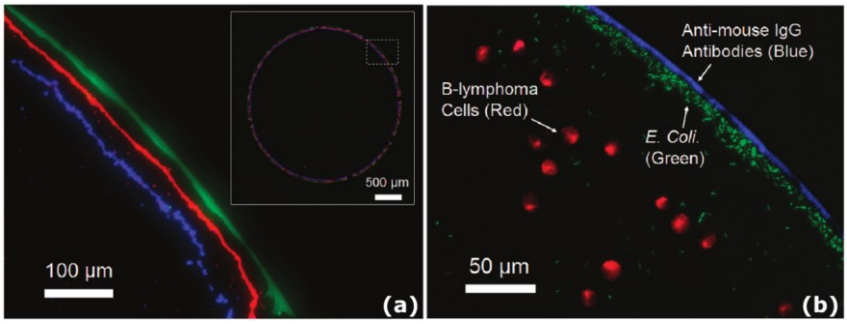

Figure 20. (a) Separation of particles with different sizes of 2 μm (blue), 1 μm (red), and 40 nm (green) after complete evaporation. (b) Separation of B-lymphoma cells (red), Escherichia

coli (green), and antimouse IgG antibodies (blue). Reprinted with permission from Ref. [128] Copyright (2011) American Chemical Society.

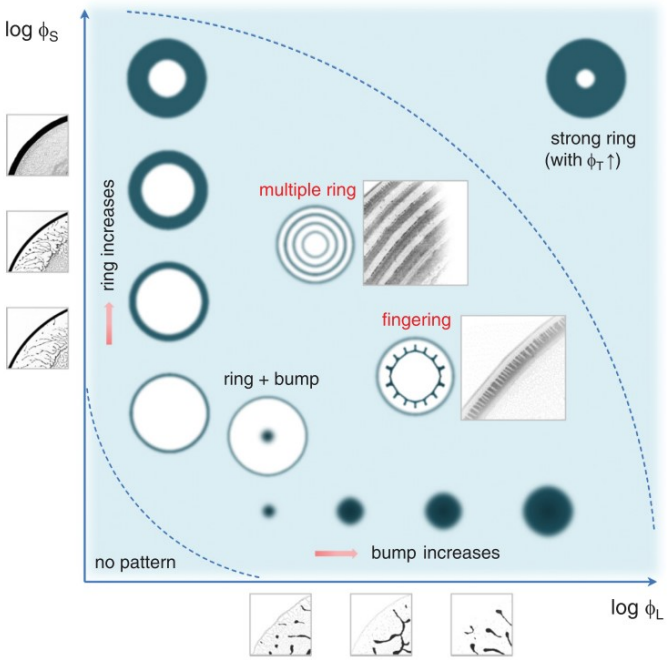

Figure 21. Schematic phase diagram of deposition patterns from monodispersed and bidispersed droplets. ϕ_L and ϕ_S are the volume fractions of large and small particles for a droplet with a fixed radius, respectively. Reprinted with permission from Ref. [96] Copyright (2013) American Physical Society.

Commented [MP11]: Answer to Comment 9d by Reviewer 1

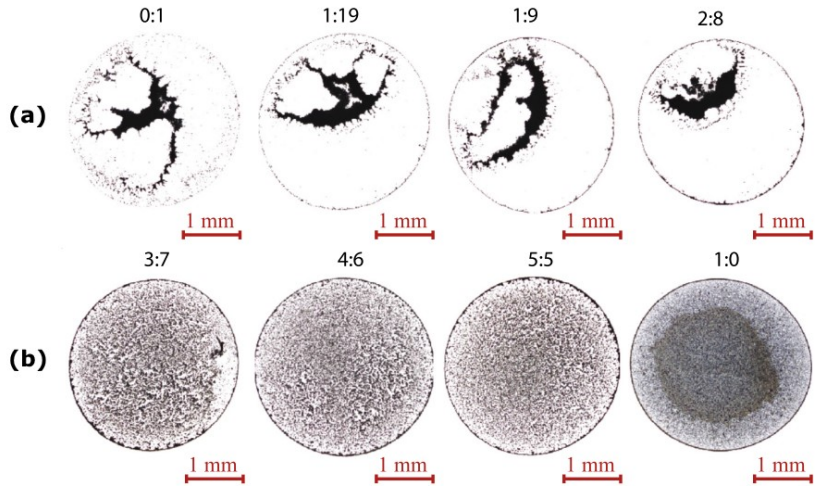

Figure 22. The deposition patterns formed by drying droplets with the weight ratio of 5-40 nm Al_2O_3 nanoparticles: (a) 0:1, 1:19, 1:9, and 2:8. (b) 3:7, 4:6, 5:5, and 1:0. Reprinted with permission from Ref. [40] Copyright (2017) Elsevier.

4.1.4. Material

Lee et al. [45] made a comparison between the deposition patterns of the 20 nm Al_2O_3 and 21 nm TiO_2 nanofluid drops at the same concentration of 0.05 vol % (Figure 23). The ring width of the Al_2O_3 nanoparticles was found to be smaller than that of TiO_2 nanoparticles. By considering the effect of different factors such as the material, size, and concentration of nanoparticles, the authors concluded that the material of nanoparticles has a less significant role on the pattern formation. As seen in Figure 24, the pattern formed by the mixture of the 5 nm graphite and the 5 nm Al_2O_3 nanoparticles is similar to the pattern of the Al_2O_3 nanoparticles [40]. However, the gap between the contact line and the centre-concentrated deposit is larger for the mixture pattern than that for the Al_2O_3 pattern. The effect of the combination of the two nanoparticles is found to be collaborative on the mixture pattern as they almost keep their position as in the patterns formed by either graphite or Al_2O_3 nanoparticles.

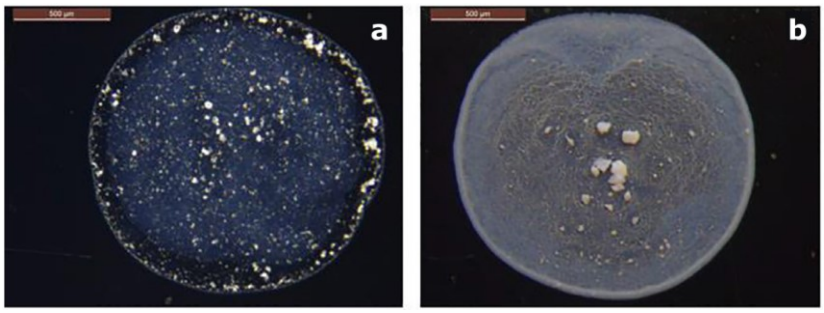

Figure 23. Deposition patterns after drying sessile drops containing different materials of nanoparticles: (a) 20 nm Al_2O_3 and (b) 21 nm TiO_2 with 0.05 vol % concentration on stainless steel. Reprinted with permission from Ref. [45] Copyright (2017) American Chemical Society.

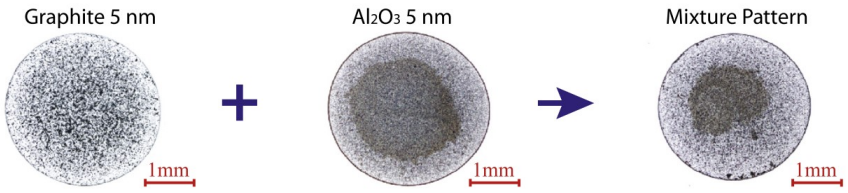

Figure 24. Deposition patterns after drying sessile drops containing single 5 nm graphite nanoparticles, the single 5 nm Al_2O_3 nanoparticles, and the mixture of graphite and Al_2O_3 nanoparticles. Reprinted with permission from Ref. [40] Copyright (2017) Elsevier.

4.2. Atmospheric conditions

Commented [MP12]: Answer to Comment 6a by Reviewer 1

4.2.1. Relative humidity

Only few studies in the literature address the effect of relative humidity on the deposition pattern. It has been found that the increase of the relative humidity decreased the evaporation rate of a drop containing particles, but increased the spreading of the drop with lower contact angle, leading to a larger deposition area [129]. The droplets followed the CCR mode during the entire evaporation for all relative humidities [9,129]. The internal flow was driven toward the contact line and formed the ring-like patterns [9,129]. The deposition patterns of dried

nanofluid drops were identical for different humidity values varying from 13 to 85% [9]. However, the increase of the relative humidity affected the dried pattern of blood drops on glass substrates [21]. The deposition pattern was characterized by three distinctive areas, as shown in Figure 25: a fine peripheral area adhering to the substrate; a coronal area composed of wide mobile plaques with radial white cracks; and, a central area composed by small cracks and a sticking deposit. By increasing the humidity, the width of the peripheral area increased which is shown in between the two yellow bars in Figure 25. The increase of the humidity decreased the contact angle, and consequently increased the diameter of the deposition pattern as well as the width of the wedge near the contact line. This leads to the formation of the wider peripheral area with increasing the humidity. By increasing the humidity from 13.5 to 50%, the size of plaques in the corona increased, but decreased by the further increase of the humidity from 50 to 78%. The difference in the size of plaques can be attributed to the evaporation rate which affects the adhesion of the drop to the substrate [22].

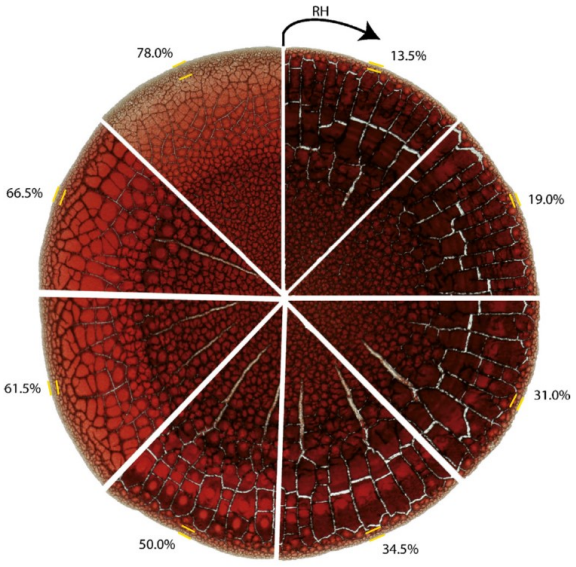

Commented [MP13]: Answer to Comment 6b by Reviewer 1 and Answer to Comment 1 by Reviewer 2

Figure 25. Influence of various range of relative humidity on the pattern formation of a sessile blood drop. Area between the two yellow bars indicates the peripheral area. Reprinted with permission from Ref. [21] Copyright (2013) Elsevier.

4.2.2. Ambient temperature and pressure

An investigation was carried out to find the effect of the environmental temperature on the deposition patterns of the dried TiO_2 and Al_2O_3 nanofluid drops [36]. At the same concentration, the deposition pattern of Al_2O_3 nanoparticles was relatively independent of the ambient temperature. However, in the case of TiO_2 nanofluid, increasing the temperature led to the ring-like pattern formation with the concentric rings in the interior of the peripheral ring.

Askounis et al. [14] investigated the influence of reduced atmospheric pressure varying from 750 to 100 mbar on the final deposition patterns left after the full evaporation of water drops containing SiO_2 nanoparticles (see Figure 26). Reducing the atmospheric pressure enhanced the evaporation rate due to the increase of the effective diffusion coefficient of water vapour in the environment. The evaporating drop followed the "stick-slip" mode under 750 mbar pressure, and hence the "stick-slip" pattern was formed (Figure 26a). However, the ring-like pattern was formed under 500 mbar pressure (Figure 26b), and a wider and thicker ring was obtained with a further reduction of pressure to 250 mbar (Figure 26c). The outward flow contributed to the accumulation of nanoparticles at the contact line and thus enhanced the pinning effect which both led to the formation of the ring-like patterns, but the thicker ring resulted from the stronger outward flow caused by the further reduction of the pressure. At 500 mbar pressure, the assembly of hexagonal, closed-packed nanoparticle structures was also observed. A different ring-like pattern with an inner irregular shape was formed under 100 mbar pressure (Figure 26d). The high deposit was brought near the edge by the very strong outward flow induced by the extremely high evaporation rate. Moreover, the fast evaporation did not give sufficient time to the fluid to flow towards the edge, and thus became frozen in

place, forming the different inner deposits from those drops under 250 and 500 mbar. From the nanoscopic point of view, nanoparticle pattern crystallinity was promoted with reducing pressure.

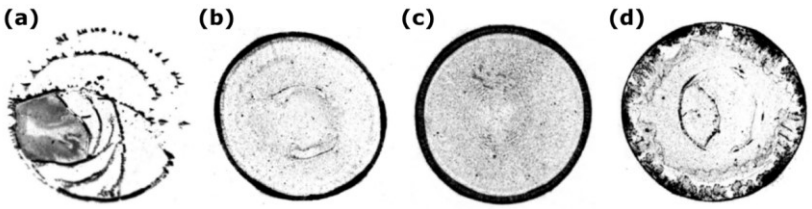

Figure 26. Influence of reduced environmental pressure on the pattern formation of a sessile SiO_2 nanofluid drop: (a) 750 mbar, (b) 500 mbar, (c) 250 mbar, and (d) 100 mbar. Reprinted with permission from Ref. [14] Copyright (2014) Elsevier.

4.3. Substrate effect

Commented [MP14]: Answer to Comment 6a by Reviewer 1

One of the most important effects on deposition patterns is related to substrate surface. The literature shows that wettability and temperature of substrates strongly influence dried patterns, but the material of substrate has less important role on deposition patterns [45]. Increasing the wettability of substrate led to the deposition of more particles in the central regions whereas decreasing the wettability promoted the formation of the ring-like pattern [45]. Moreover, increasing the wettability contributed to a better size sorting in drying bidispersed droplets [41]. It was also found that the lowering the contact angle hysteresis (CAH) could supress the coffee-rig effect and led to the deposition of the dot-like patterns instead of the ring-like patterns [42].

The study of substrate temperature has received much attention in the past four years. The internal flow is strongly affected by substrate temperature which plays a key role in the pattern formation of particles. Non-isothermally heated substrates created different patterns from isothermally heated substrates [130]. Increasing hydrophilic substrate temperature led to the transition from the ring-like pattern with the inner uniform deposition to either the dual-ring

pattern or inner deposits enclosed with the peripheral ring [15,47]. However, increasing hydrophobic substrate temperature led to the transition from the dot-like pattern to the inner deposit inside the peripheral ring [44].

Commented [MP15]: Answer to Comment 1 by Reviewer 2

4.3.1. Wettability of substrate

It was previously mentioned that it is more likely to observe the coffee-ring pattern on the hydrophilic or high wettability substrates. Contrarily, the dot-like pattern or central-like deposits are more likely to form on hydrophobic or less wettability substrates. Lee et al. [45] studied the influence of different substrate materials on deposition patterns of nanofluid droplets by using glass, stainless steel, and Teflon surfaces with the initial contact angles of 55.2°, 80.9°, and 90.4°, respectively. The authors confirmed that it was easier for drying droplets to form a ring-like pattern on the high wettability substrate with lower contact angle. On the other hand, more nanoparticles were found in the centre of the peripheral ring on less wettability substrate with larger contact angle. For example, more nanoparticles concentrated in the centre of the pattern formed on stainless steel compared to that formed on glass. This was attributed to the droplet shape as it is affected by the contact angle. A droplet with larger contact angle has greater height at the centre and smaller base diameter, thereby more nanoparticles should be found in the central region after the complete evaporation. A droplet with low contact angle has smaller height at the centre and larger base diameter which enhances the evaporation rate as well as the flow velocity. This makes it easier for the droplet to form a ring-like pattern. By considering the other factors such as particle size, particle concentration, etc., the effect of substrate material was found to be less significant on the final deposition patterns [45]. However, several studies have shown that the wettability of the substrate plays an important role on the drying process and thus final deposition patterns [42,44,59]. As an example, Orejon et al. [59] studied the effect of nanoparticles presence on the dynamics of the contact line on substrates of various hydrophobicities, and observed the “stick-slip” behaviour

only on hydrophobic substrates. Chhasatia and Sun [41] investigated the substrate wettability on the pattern formation of droplets containing bidispersed particles. On the substrates with higher wettability, particles of different sizes were further separated than those on the substrates with lower wettability. This was attributed to the effects of the different evaporation modes, the substrate-particle interactions, the surface tension and drag forces acting on particles on the rearrangement of particles near the contact line during evaporation. Jeong et al. [43] showed that the separation of nano- and microparticles near the contact line only occurred on hydrophilic substrates. Conversely, hydrophobic substrates could not separate the suspended particles as the contact line was not pinned and receded during evaporation. Li et al. [42] demonstrated that the final deposition pattern of polymer particles could be manipulated by controlling contact angle hysteresis (CAH). Ring-like patterns were formed on substrates with strong CAH such as poly(vinyl pyrrolidone) (Figure 27a), and dot-like patterns were formed on substrates with weak CAH such as sodium polysulfonate (Figure 27b). Very recently, Zhong et al. [46] investigated the effect of various substrates on crystal patterns from saline droplets (see Figure 28). Cubic crystals were formed at the centre of the dried droplet deposited on silicon and PMMA substrates with the lower wettability and the weaker pinning effect. However, the high wettability and the stronger pinning effect of the soda lemon glass result in the formation of a spherical profile composed of thin layer of salt and cubic crystals.

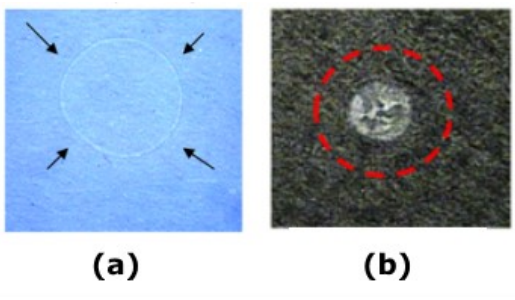

Figure 27. Deposition patterns of polymer particles on substrates with different values of contact angle hysteresis (CAH): (a) Strong CAH and (b) Weak CAH. Reprinted with permission from Ref. [42] Copyright (2013) American Chemical Society.

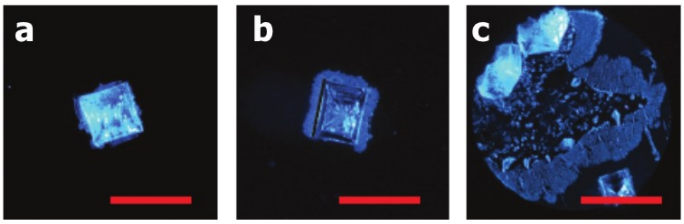

Figure 28. Dried deposits of saline droplets containing 10 % salt on: (a) Silicon wafer, (b) PMMA, and (c) Soda lemon glass. Scale bar, 1 mm. Reprinted with permission from Ref. [46] Copyright (2017) American Chemical Society.

4.3.2. Substrate temperature

Substrate temperature is a key factor in the sessile drop evaporation process and thus the final deposition pattern. It was found that the change of the substrate temperature could change the flow direction at the late stages of the evaporation, and thus the dried deposition patterns of water-polymer droplets were different on the heated substrate from the cooled one [66]. The evaporation of a poly(ethylene oxide) (PEO) droplet formed a "puddle" structure on the isothermally heated substrate at 30 °C [130]. However, a peculiar "dual-ring" structure was left behind after the full evaporation on the non-isothermally heated substrate at the rate of 20 °C/min. At lower temperatures, the capillary flow was dominant and led to the formation of the peripheral ring. The further increase of temperature increased the surface stress gradient and decreased the viscous stress, resulting in the contact line recession. Eventually, the Marangoni flow became dominant at the late stages of the evaporation process, forming the "dual-ring" structure. Hendarto and Gianchandani [131] investigated the influence of the substrate temperature on the size sorting of hollow glass spheres with different diameters (from

5 to 200 μm) inside drying isopropyl-based droplets. The authors demonstrated that most of the larger spheres (150–200 μm) deposited in the central regions of the droplet at the substrate temperature of 55 °C, but the smaller spheres (<50 μm) deposited in different regions of the dried droplet. At the substrate temperature above the boiling point of the base fluid (85 °C), most of the smaller particles were found near the droplet edge, leading to better size sorting. Parsa et al. [15] studied the influence of a wide range of hydrophilic substrate temperatures varying from 25 to 99 °C on the pattern formation of nanofluid droplets. They found three distinctive deposition patterns, as shown in Figure 29: a relatively uniform pattern, "dual-ring" pattern, and "stick-slip" pattern. On the non-heated substrate, the outward flow was dominant and formed a ring-like pattern with a relatively uniform deposition of nanoparticles inside the peripheral ring (Figure 29a). On the substrates heated between 47 and 81 °C, the outward flow carried nanoparticles towards the edge, and helped to form a peripheral ring. Meanwhile, there were a group of nanoparticles that moved towards the edge but did not deposit there due to the existence of a stagnation point at the free interface where the surface flow change the direction (Figure 30). These repelled nanoparticles returned back along the free interface of the drop due to the presence of an inward Marangoni flow caused by the temperature gradient along the interface. These nanoparticles collected at the top of the free surface of the drop and built a ring-like cluster of nanoparticles there. This cluster deposited in the interior region of the droplet when it reached the depinning contact line, leading to the formation of a secondary ring enclosed with the peripheral ring (Figure 29b-d). The distance between the secondary and peripheral ring decreased with increasing temperature. At temperature of 99 °C, the same internal flow structure was observed, but the "stick-slip" of the contact line at the end of the evaporation prevented the ring-like cluster from depositing as the secondary ring inside the peripheral ring, and consequently the "stick-slip" pattern was formed on the substrate (Figure 29e). Following the study of Parsa et al. [15], several works have been published related to the

influence of substrate temperature on the evaporation and the final deposition pattern [44,47,48,132,133]. Li et al. [47] reported the deposition of "eye-like" patterns after the evaporation of colloidal droplets on heated substrates of low thermal conductivity. A thermally-driven Marangoni flow was found to be the main mechanism for the formation of this pattern which was the combination of a thin peripheral ring with an inner dot-like deposit at the centre of the droplet. Zhong et al. [132] observed an indistinct "dual-ring" pattern after the drying of nanofluid droplets on the substrate at room temperature. The "dual-ring" pattern disappeared with the further increase of the substrate temperature, and instead a single ring pattern was formed. The inward Marangoni flow was intensified with enhancing the temperature, and carried nanoparticles along the free interface which sharpened the inner ring. At the same time, the enhanced capillary flow expanded the inner ring and merged it with the outer ring. Zhong and Duan [48] reported the transition from a disk-like pattern with the inner uniform coverage to the "dual-ring" pattern from cooled to heated the substrate. Droplets on the cooler substrate than the surrounding environment showed three stages of evaporation. During the first two stages, a majority number of nanoparticles either formed the peripheral coffee-ring or deposited in the interior region, making an annular gap between them. During the last stage, the gap was filled by the nanoparticles moved towards the contact line. Above the transition temperature, the co-occurrence of the inward Marangoni and capillary flows led to the formation of the "dual-ring" pattern. In the recent study by Patil et al. [44], the influence of substrate temperature on the pattern formation of particles for hydrophobic substrates was investigated. As expected, on non-heated substrates, an inner deposit stain with no peripheral ring was observed (Figure 31a), but on heated substrates, a combined pattern consisting of an inner deposit and a coffee-ring pattern was formed (Figure 31b,c). Heating the substrate made a delay in the depinning of the contact line, and also the transition from the CCR mode to the CCA one. The drying process occurred mostly in the CCR mode caused by the self-pinning of particles in the stagnation

region which is divided in an outward and Marangoni flows. As a result of this self-pinning, the thin coffee-ring pattern formed on the heated substrate with the inner deposit inside the ring. Moreover, Increasing the substrate temperature increased the height of the ring which was attributed to higher Marangoni velocity and larger contact angle.

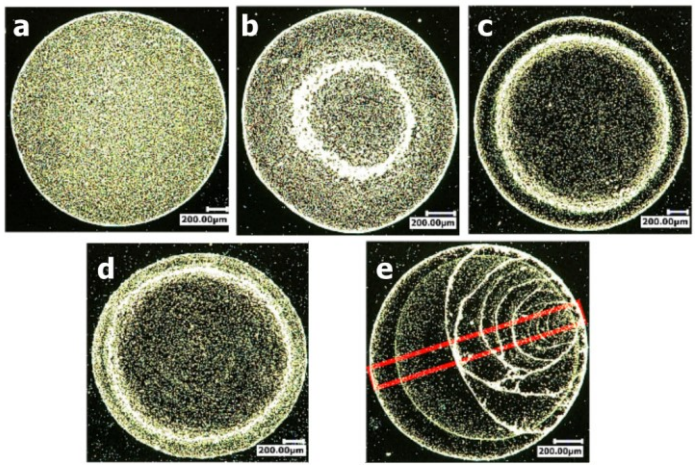

Figure 29. Influence of hydrophilic substrate temperature on pattern formation of CuO nanofluid drops: (a) 22 °C, (b) 47 °C, (c) 64 °C, (d) 81 °C, and (e) 99 °C. Reprinted with permission from Ref. [15] Copyright (2015) American Chemical Society.

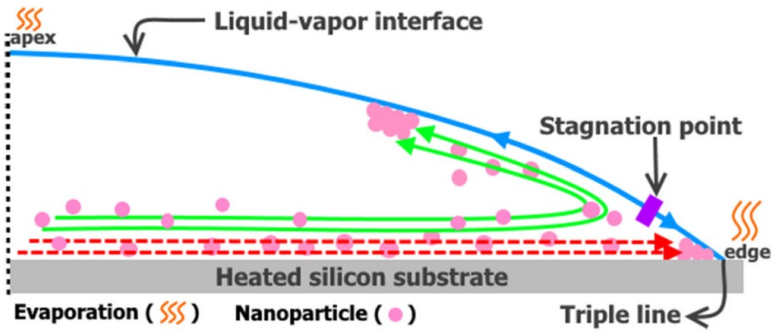

Figure 30. Stagnation point at the free interface of a drying drop. The solid arrows indicate the Marangoni flows. The dashed arrows indicate the outward flow. Reprinted with permission from Ref. [13] Copyright (2017) Springer.

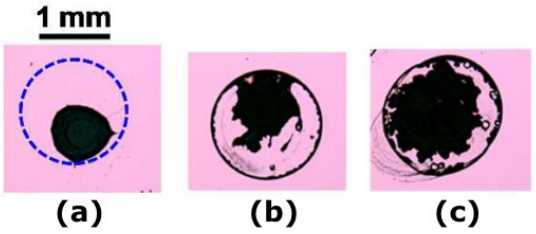

Figure 31. Influence of hydrophobic substrate temperature on pattern formation after drying drops with particle concentration of 1 vol %: (a) 27.5 °C, (b) 60 °C, and (c) 90 °C. The dashed line indicates the initial contact line. Reprinted with permission from Ref. [44] Copyright (2016) American Chemical Society.

4.4. Base fluid

Base fluid plays an important role in the formation of deposition patterns. There are two main ways to make changes in base fluid to manipulate the morphology of an evaporating droplet. One is the addition of surfactants into base fluid; and the other is manipulating the chemical composition of base fluid. Surfactants affect the inner flows, the contact line motion, interparticle interactions, etc. The relevant studies showed that different deposition patterns can be created depending on the type of surfactants used in base fluid. Biosurfactants, ionic surfactant sodium dodecyl sulfate (SDS), and polymer-like surfactants altered the coffee-ring effect, thus inhibiting the formation of the coffee-ring pattern [10,61,81]. On the other hand, cetyltrimethylammonium bromide (CTAB) surfactant contributed to the formation of the coffee-ring pattern [134].

The effect of fluid composition on the deposition patterns strongly depends on properties and/or contents of each liquid in composition (in the case of binary solution). These factors can significantly affect the internal flow and the evaporative dynamics. The base fluid with higher viscosity formed the coffee-ring pattern, whereas that with lower viscosity formed a more uniform pattern [115]. Depending on the concentration of liquids used in a binary-based droplet, different deposition patterns can be formed. For a drying ethylene glycol-water droplet, there was a transition from a uniform pattern to a ring-like pattern by increasing ethylene glycol contents [135]. However, the literature shows differences in the results related to the dried patterns left after a drying ethanol-water droplet. One study reported that the increase of ethanol content promoted the formation of the ring-like pattern [135], whereas the other study showed the uniformity of the deposition was promoted by increasing ethanol [11]. However, the further increase led to the detachment of the inner uniform deposition from the outer ring. These differences in the studies may be attributed to the effect of other key factors which are not the same during the experiments such as solute (i.e. concentration, size, material), substrate, etc.

Commented [MP16]: Answer to Comment 8 by Reviewer 1 and Answer to Comment 1 by Reviewer 2

4.4.1. Surfactants

Adding surfactants into base fluid is another way to alter the deposition pattern of drying sessile drops. The addition of ionic surfactant sodium dodecyl sulfate (SDS) significantly altered the coffee-ring effect inside an evaporating colloidal drop [10]. A strong inward Marangoni flow was created by SDS along the air-liquid interface of the drop that prevents most of particles from depositing at the contact line, forming a more uniform deposition pattern. Similarly, biosurfactants generated a surface tension gradient along the air-liquid interface, inducing a Marangoni flow [61]. The particles moved towards the drop edge but did not deposit there and returned back inward along the free surface due to the Marangoni flow. Hence, the coffee-ring effect was inhibited and the particles were uniformly distributed on the substrate (Figure 32). Seo et al. [81] made a comparison between the pattern deposition of SDS

(surfactant) and surfactant-like polymer solutions. Both the two surfactants altered the coffee-ring effect and lead to the formation of multiple ring patterns. However, the rings formed by the surfactant-like polymer were more uniform due to the change of the depinning and receding of the contact line caused by the characteristics of the surfactant. The depinning of the contact line for the surfactant-like polymer was easier as it required less force. Therefore, smaller distance between each ring were observed and more uniform multiple rings were left after the full evaporation. Contrary to the aforementioned studies, the addition of cetyltrimethylammonium bromide (CTAB) surfactant into graphite nanofluid drops promoted the coffee-ring effect, and formed the coffee-ring pattern instead of the uniform one, as shown in Figure 33 [134]. The same transition from the uniform pattern to the coffee-ring pattern was observed after adding CTAB surfactant into Al_2O_3 nanofluid drops [136]. A 2D diffusion limited cluster−cluster aggregation (DLCA) method was used to explain the transition. The simulation showed that the interparticle sticking probability has a significant influence on the pattern formation.

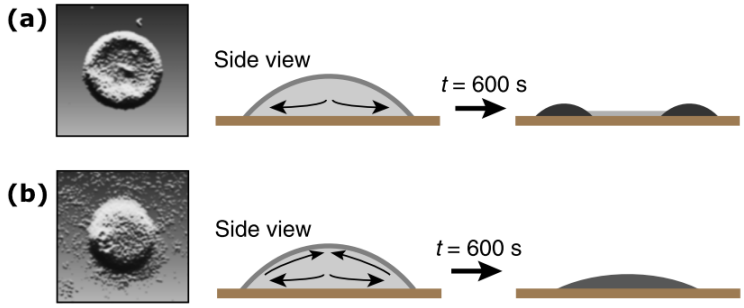

Figure 32. A coffee-ring pattern was formed without biosurfactants due to the coffee-ring effect. (b) A uniform pattern was formed with biosurfactants due to the strong Marangoni flow. Reprinted with permission from Ref. [61] Copyright (2013) Nature Publishing Group.

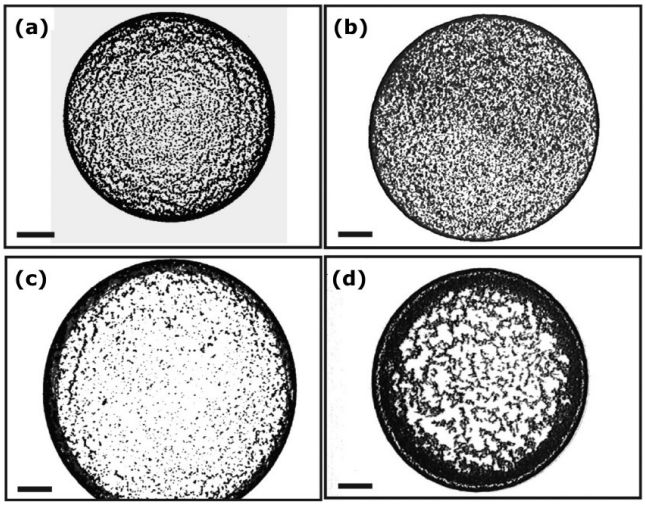

Figure 33. Deposition patterns left after full evaporation of graphite nanofluid drops: (a) At concentration of 2 g/L without the CTAB surfactant. (b) At concentration of 5 g/L without the CTAB surfactant. (c) At concentration of 2 g/L with the CTAB surfactant. (d) At the concentration of 5 g/L with the CTAB surfactant. Reprinted with permission from Ref. [134] Copyright (2013) American Chemical Society.

4.4.2. Fluid composition

It is noteworthy that pure water has been widely used as the base fluid in the studies relevant to the pattern formation from sessile drops. Change in the base fluid composition can be a way to control the particle deposition morphology of a drying colloidal droplet. As an example, Choi et al. [115] made a comparison between the effect of Newtonian and non-Newtonian base fluids on the pattern formation of 6 μm polystyrene particles suspended in aqueous solutions of water, PEO, and xanthan gum (XG). The evaporation of XG solution formed the coffee-ring pattern, while a more inner uniform pattern with no distinct ring was formed after the evaporation of water and PEO solutions. The difference in the deposition patterns observed between the PEO and XG solutions was attributed to the difference between their viscosities.

The viscosity of the XG solution remains high during low shear drying as it has a very high zero shear viscosity. For higher viscosity fluids, the capillary flow transport more particles towards the drop edge at the early stages of the evaporation, and thus leading to the formation of the coffee ring pattern. Talbot et al. [135] studied deposition patterns from drying colloidal droplets influenced by two binary base fluids of water-ethylene glycol and water-ethanol. Uniform patterns enclosed with thick rings were formed at low concentration (10 and 30 vol %) of ethylene glycol in water, as shown in Figure 34. At higher concentration of ethylene glycol (50 – 90 vol %), ring-like patterns were formed with the less dense interior regions. For concentrations above 70 vol %, unfilled regions were also observed inside the peripheral rings. Ethylene glycol-water mixture droplets showed rapid particle movement toward the contact line as water evaporates first. When ethylene glycol dominated the drying process, particle movement slowed down but still remained radially outward. At high concentration of ethylene glycol (i.e., 90 vol %), no inward Marangoni flow was observed, thus a slow radial flow dominated the evaporation, leading to the formation of the rings. For low concentration of ethylene glycol (i.e., 10 vol %), there was a more rapid outward flow during the evaporation process dominated by water. Afterwards, during the ethylene glycol dominated evaporation, the outward flow slowed down without Marangoni flow. The uniform coverage could not be fully explained by the inner flow. The uniform coverage inside the rings was attributed to particles that did not have enough time to reach the edge after the transition to the evaporation process dominated by ethylene glycol, along with the increased particle concentration from large volume loss. Drying water-ethanol binary-based droplets formed ring-like deposits. The width of the rings increased with increasing ethanol concentration from 10 to 90 vol %. At the beginning of evaporation for the ethanol concentrations between 10 – 50 vol %, inner flows showed particles collected at the central regions until the drying process was dominated by water. Then, the radial outward flow dominated the flow field. At ethanol concentration of 90

Commented [MP17]: Answer to Comment 7a by Reviewer 1

Commented [MP18]: Answer to Comment 7b by Reviewer 1

vol %, the flow slowed down, and lower contact angle facilitated pinning of the contact line, forming a ring-like deposit. As shown in Figure 35, the deposition patterns of water-ethanol binary-based nanofluid droplets are affected by the ethanol concentration [11]. The evaporation of pure water-based suspension formed a nearly uniform pattern (Figure 35a). However, at the ethanol concentration of 10 vol %, most nanoparticles deposited in the centre of the droplet and detached from the peripheral ring (Figure 35b). The dried pattern showed uniformity again as the ethanol concentration increased to 25 vol % (Figure 35c). However, the inner deposit started to detach from the peripheral ring with a further increase of the ethanol concentration to 40 and 50 vol % (Figure 35d,e). Parsa et al. [13] studied the deposition patterns of binary water-butanol CuO nanofluid droplets and compared with those of pure water-based CuO nanofluid droplets at the same substrate temperatures. Adding 5 wt % butanol into the base fluid did not significantly affect the deposition patterns (Figure 36). Similar to the patterns observed for the water-based droplets (Figure 29) [15], the nearly uniform pattern was formed on the non-heated substrate (Figure 36a), the "dual-ring" patterns for heated substrate temperatures from 47 to 81 °C (Figure 36b-d), and the "stick-slip" pattern for substrate temperature of 99 °C (Figure 36e). However, the distribution of nanoparticles was found to be different in the central regions as the several inner faint lines were observed inside the secondary ring of the "dual-ring" patterns. Strong and chaotic vortices appeared from the beginning of the evaporation and transported nanoparticles to the air-liquid interface. Then, the flow slowed down and these nanoparticles stayed at the free interface. A fraction of these nanoparticles contributed to the formation of a ring-like cluster on the top region of the droplet, while the remainders stay inside the ring-like cluster at the interface. Moreover, the thermal Marangoni flow carried nanoparticles towards the top region of the droplet along the air-liquid interface which helps to build the ring-like cluster. Meanwhile, a group of nanoparticles adjacent to the substrate was carried towards the contact line and formed the peripheral ring.

After the depinning of the contact line, those nanoparticles enclosed with the ring-like cluster at the interface deposited on the substrate and formed the inner faint lines in the secondary ring.

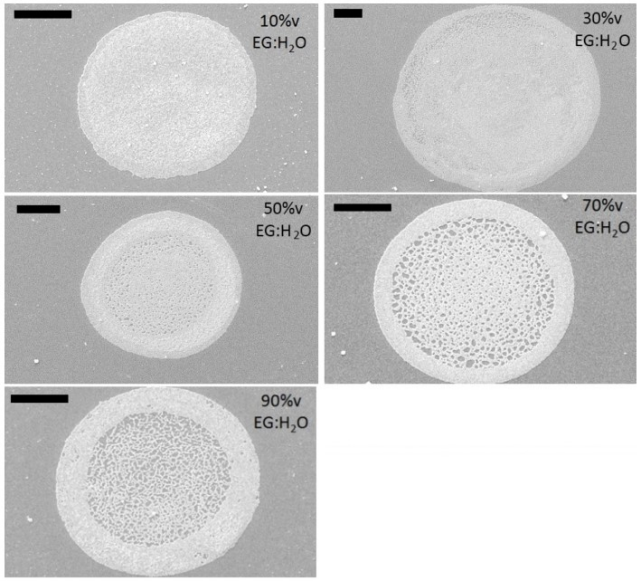

Figure 34. Deposition patterns from ethylene glycol-water binary-based droplets containing 1 vol % 220 nm spheres (Scale bar 20 μm). Reprinted with permission from Ref. [135] Copyright (2012) Society for Imaging Science and Technology.

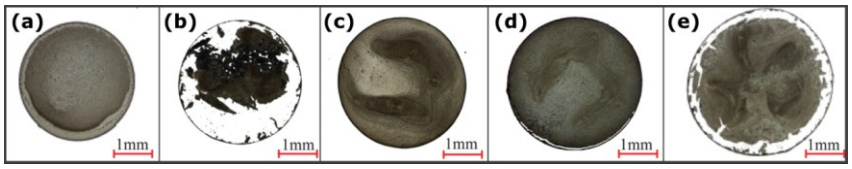

Figure 35. Influence of the ethanol concentration on the pattern formation of 1.5 g/L graphite-water nanofluid droplets: (a) 0 vol %, (b) 10 vol %, (c) 25 vol %, (d) 40 vol %, and (e) 50 vol %. Reprinted with permission from Ref. [11] Copyright (2014) American Chemical Society.

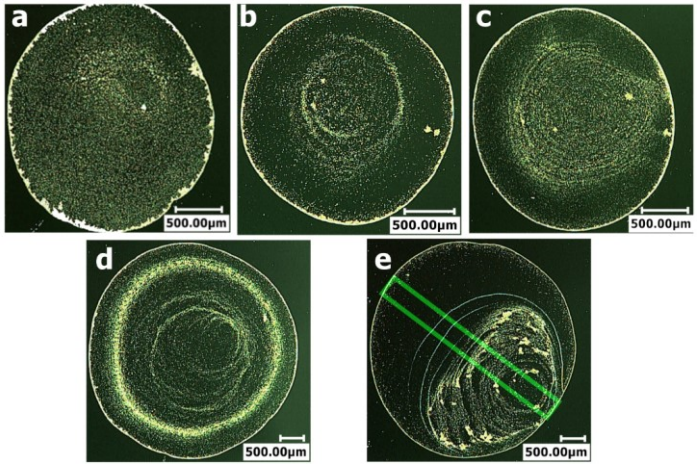

Figure 36. Dried patterns left after the evaporation of butanol-water based nanofluid droplets at different substrate temperatures: (a) 25 °C, (b) 47 °C, (c) 64 °C, (d) 81 °C, and (e) 99 °C. Reprinted with permission from Ref. [13] Copyright (2017) Springer.

4.5. Electrowetting

In the previous sections, the droplets evaporated freely and the deposition patterns were formed naturally. Another efficient way to manipulate the deposition patterns is to apply electrowetting with a voltage to colloidal droplets. Eral et al. [137] showed that an alternating current (AC) electrowetting suppressed the coffee-ring effect of droplets of different particle sizes and DNA solutions. As shown in Figure 37a-c, at frequencies of 6 Hz and 1 kHz, the electrowetting prevented the pinning of the contact line and generated the internal flow which counteracted the evaporation driven flux, and thus did not allow the particles to deposit at the contact line. However, at higher frequency of 100 kHz (Figure 37d), the electrowetting led to less pronounced coffee-ring pattern, but did not form a dot-like pattern similar to what was observed for lower frequencies of 6 Hz and 1 kHz. This problem was eliminated by applying the amplitude modulation of the high frequency (100 kHz) with the low one (100 Hz), resulting in the formation of a very small dot-like pattern (Figure 37e). The electrokinetic mechanisms

for a droplet under AC conditions can differ from those applied under direct current (DC) conditions [138]. Orejon et al. [138] studied the evaporation of TiO_2 nanofluid droplets under a DC potential. The "stick-slip" behaviour of droplets was suppressed, and instead the contact line receded monotonically for most of evaporation time. Nanoparticles preferentially moved towards the substrate by electrophoretic forces instead of arriving at the contact line, and thereby more uniform patterns were formed.

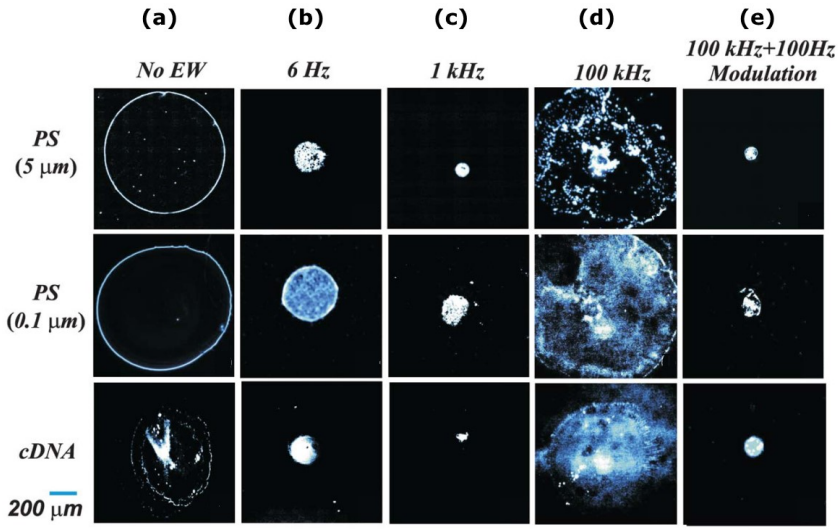

Figure 37. Influence of AC electrowetting (EW) on the pattern formation of colloidal droplets of different particle sizes and DNA solutions. Reprinted with permission from Ref. [137] Copyright (2011) Royal Society of Chemistry.

5. Limitations of study

Even though pattern morphologies of drops have a wide range of applications, there are limitations in the reviewed studies which make the comparisons complicated. While studying the effect of a single factor on desiccation patterns from droplets, they are sensitive to many other factors which are different from one study to another. In some cases, this leads to some

controversies in the comparisons. As an example, for the effect of solute concentration, the other factors such as substrate, size, and material of solute are not identical in the studies. Hence, the effect of some factors (i.e., solute concentration, fluid composition) on patterns remain controversial. For a group of factors (e.g. solute shape, material, atmospheric conditions), the studies are still in a very early stage as there are only few studies in which the other factors (e.g. size and material of solute) are not identical and may lead to draw incorrect conclusions. For those studies with the medical applications (i.e., diseases diagnosis), it has been shown that the environmental conditions (i.e., relative humidity) affect the dried patterns of blood drops. Thus, it is of highly importance that the diagnosis tests are needed to be carried out under the controlled environmental conditions.

Commented [MP19]: Answer to the editor's comments about the limitations.

6. Conclusion

It is obvious that the evaporation of a droplet containing particles and consequently its pattern formation of particles is dependent on a wide range of factors such as solute, environmental conditions, base fluid, etc. This literature review clearly shows the interest of researchers in the experimental study of the driving factors that lead to a variety of deposition patterns. Despite this, because the evaporation of a droplet without particles remains a complex phenomenon, the full understanding of pattern formation from droplets of complex fluids is still lacking and more research is needed to be done to explain mechanisms behind the final patterns. In this review, the effects of key factors on desiccation patterns are elucidated which have not been mentioned or not extensively discussed in the previous review papers. Some of these factors are wettability of substrate, substrate temperature, chemical fluid composition, mixing particles with different properties, sizes, and shapes, etc. This review paper suggests that the forthcoming studies might be on pattern formation from evaporating colloidal droplets of different liquids deposited onto non-isothermally heated substrates with various wettability.

Acknowledgement

This work has been achieved within the framework of CE2I project (Convertisseur d'Énergie Intégré Intelligent). CE2I is co-financed by European Union with the financial support of European Regional Development Fund (ERDF), French State and the French Region of Hauts-de-France.

References

[1] N. Gudris, L. Kulikowa, Die verdampfung kleiner wassertropfen, Zeitschrift Für Phys. 25 (1924) 121–132. doi:10.1007/BF01327514.

[2] R.F. Mangel, E. Baer, The evaporation of water drops from a "Teflon" surface, Chem. Eng. Sci. 17 (1962) 705–706. doi:10.1016/0009-2509(62)85029-5.

[3] R.D. Deegan, O. Bakajin, T.F. Dupont, G. Huber, S.R. Nagel, T.A. Witten, Capillary flow as the cause of ring stains from dried liquid drops, Nature. 389 (1997) 827–829. doi:10.1038/39827.

[4] R. Deegan, O. Bakajin, T. Dupont, G. Huber, S. Nagel, T. Witten, Contact line deposits in an evaporating drop, Phys. Rev. E. 62 (2000) 756–765. doi:10.1103/PhysRevE.62.756.

[5] R.D. Deegan, Pattern formation in drying drops, Phys. Rev. E. 61 (2000) 475–485. doi:10.1103/PhysRevE.61.475.

[6] K. Sefiane, Patterns from drying drops., Adv. Colloid Interface Sci. 206 (2014) 372–81. doi:10.1016/j.cis.2013.05.002.

[7] X. Zhong, A. Crivoi, F. Duan, Sessile nanofluid droplet drying, Adv. Colloid Interface Sci. 217 (2015) 13–30. doi:10.1016/j.cis.2014.12.003.

[8] C.H. Chon, S. Paik, J.B. Tipton, K.D. Kihm, Effect of nanoparticle sizes and number

densities on the evaporation and dryout characteristics for strongly pinned nanofluid droplets, Langmuir. 23 (2007) 2953–2960. doi:10.1021/la061661y.

[9] D. Brutin, Influence of relative humidity and nano-particle concentration on pattern formation and evaporation rate of pinned drying drops of nanofluids, Colloids Surfaces A Physicochem. Eng. Asp. 429 (2013) 112–120. doi:10.1016/j.colsurfa.2013.03.012.

[10] T. Still, P.J. Yunker, A.G. Yodh, Surfactant-induced Marangoni eddies alter the coffee-rings of evaporating colloidal drops, Langmuir. 28 (2012) 4984–4988. doi:10.1021/la204928m.

[11] X. Zhong, F. Duan, Evaporation of sessile droplets affected by graphite nanoparticles and binary base fluids, J. Phys. Chem. B. 118 (2014) 13636–13645. doi:10.1021/jp508051y.

[12] M. Parsa, S. Harmand, K. Sefiane, M. Bigerelle, Evaporation of binary mixture nanofluid drops: Pattern formation, in: M. Laudon, F. Case, B. Romanowicz (Eds.), 10th Annu. TechConnect World Innov. Conf., TechConnect, Washington, 2016: pp. 196–197. http://www.techconnect.org/proceedings/paper.html?volume=TCB2016v3&chapter=6&paper=752.

[13] M. Parsa, R. Boubaker, S. Harmand, K. Sefiane, M. Bigerelle, R. Deltombe, Patterns from dried water-butanol binary-based nanofluid drops, J. Nanoparticle Res. 19 (2017) 268. doi:10.1007/s11051-017-3951-2.

[14] A. Askounis, K. Sefiane, V. Koutsos, M.E.R. Shanahan, The effect of evaporation kinetics on nanoparticle structuring within contact line deposits of volatile drops, Colloids Surfaces A Physicochem. Eng. Asp. 441 (2014) 855–866.

doi:10.1016/j.colsurfa.2012.10.017.

[15] M. Parsa, S. Harmand, K. Sefiane, M. Bigerelle, R. Deltombe, Effect of substrate temperature on pattern formation of nanoparticles from volatile drops, Langmuir. 31 (2015) 3354–3367. doi:10.1021/acs.langmuir.5b00362.

[16] E.G. Rapis, Soviet technical physics letters, 14 (1988) 679.

[17] E. Rapis, A change in the physical state of a nonequilibrium blood plasma protein film in patients with carcinoma, Tech. Phys. 47 (2002) 510–512. doi:10.1134/1.1470608.

[18] V.N. Shabalin, S.N. Shatokhina, Method of diagnosing complicated urolithiasis and prognosticating urolithiasis, EP0504409 B1, 1996.

[19] H.M. Gorr, J.M. Zueger, D.R. McAdams, J.A. Barnard, Salt-induced pattern formation in evaporating droplets of lysozyme solutions, Colloids Surfaces B Biointerfaces. 103 (2013) 59–66. doi:10.1016/j.colsurfb.2012.09.043.

[20] D. Brutin, B. Sobac, B. Loquet, J. Sampol, Pattern formation in drying drops of blood, J. Fluid Mech. 667 (2011) 85–95. doi:10.1017/S0022112010005070.

[21] W. Bou Zeid, D. Brutin, Influence of relative humidity on spreading, pattern formation and adhesion of a drying drop of whole blood, Colloids Surfaces A Physicochem. Eng. Asp. 430 (2013) 1–7. doi:10.1016/j.colsurfa.2013.03.019.

[22] W. Bou Zeid, J. Vicente, D. Brutin, Influence of evaporation rate on cracks' formation of a drying drop of whole blood, Colloids Surfaces A Physicochem. Eng. Asp. 432 (2013) 139–146. doi:10.1016/j.colsurfa.2013.04.044.

[23] W. Bou-Zeid, D. Brutin, Effect of relative humidity on the spreading dynamics of sessile

drops of blood, Colloids Surfaces A Physicochem. Eng. Asp. 456 (2014) 273–285. doi:10.1016/j.colsurfa.2014.05.004.

[24] R. Chen, L. Zhang, D. Zang, W. Shen, Blood drop patterns: Formation and applications, Adv. Colloid Interface Sci. 231 (2016) 1–14. doi:10.1016/j.cis.2016.01.008.

[25] S.U.S. Choi, J.A. Eastman, Enhancing thermal conductivity of fluids with nanoparticles, in: ASME Int. Mech. Eng. Congr. Expo., ASME, San Fransisco, 1995: pp. 99–105.

[26] C.T. Nguyen, G. Roy, C. Gauthier, N. Galanis, Heat transfer enhancement using Al2O3–water nanofluid for an electronic liquid cooling system, Appl. Therm. Eng. 27 (2007) 1501–1506. doi:10.1016/j.applthermaleng.2006.09.028.

[27] J. Barber, D. Brutin, L. Tadrist, A review on boiling heat transfer enhancement with nanofluids., Nanoscale Res. Lett. 6 (2011) 1–16. doi:10.1186/1556-276X-6-280.

[28] R.A. Taylor, P.E. Phelan, T.P. Otanicar, C.A. Walker, M. Nguyen, S. Trimble, R. Prasher, Applicability of nanofluids in high flux solar collectors, J. Renew. Sustain. Energy. 3 (2011) 23104. doi:10.1063/1.3571565.

[29] D. Peer, J.M. Karp, S. Hong, O.C. Farokhzad, R. Margalit, R. Langer, Nanocarriers as an emerging platform for cancer therapy, Nat. Nanotechnol. 2 (2007) 751–760. doi:10.1038/nnano.2007.387.

[30] M.J. Kao, C.H. Lo, T.T. Tsung, Y.Y. Wu, C.S. Jwo, H.M. Lin, Copper-oxide brake nanofluid manufactured using arc-submerged nanoparticle synthesis system, J. Alloys Compd. 434–435 (2007) 672–674. doi:10.1016/j.jallcom.2006.08.305.

[31] H. Sirringhaus, T. Kawase, R.H. Friend, T. Shimoda, M. Inbasekaran, W. Wu, E.P. Woo, High-resolution inkjet printing of all-polymer transistor circuits, Science (80-.). 290

(2000) 2123–2126. doi:10.1126/science.290.5499.2123.

[32] T. Kawase, H. Sirringhaus, R.H. Friend, T. Shimoda, Inkjet printed via-hole interconnections and resistors for all-polymer transistor circuits, Adv. Mater. 13 (2001) 1601–1605. doi:10.1002/1521-4095(200111)13:21<1601::AID-ADMA1601>3.0.CO;2-X.

[33] B.J. De Gans, P.C. Duineveld, U.S. Schubert, Inkjet printing of polymers: State of the art and future developments, Adv. Mater. 16 (2004) 203–213. doi:10.1002/adma.200300385.

[34] B. Dan, T.B. Wingfield, J.S. Evans, F. Mirri, C.L. Pint, M. Pasquali, I.I. Smalyukh, Templating of self-alignment patterns of anisotropic gold nanoparticles on ordered SWNT macrostructures, ACS Appl. Mater. Interfaces. 3 (2011) 3718–3724. doi:10.1021/am2009019.

[35] T. Yakhno, Salt-induced protein phase transitions in drying drops., J. Colloid Interface Sci. 318 (2008) 225–30. doi:10.1016/j.jcis.2007.10.020.

[36] K. Sefiane, On the formation of regular patterns from drying droplets and their potential use for bio-medical applications, J. Bionic Eng. 7 (2010) S82–S93. doi:10.1016/S1672-6529(09)60221-3.

[37] P.J. Yunker, T. Still, M.A. Lohr, A.G. Yodh, Suppression of the coffee-ring effect by shape-dependent capillary interactions, Nature. 476 (2011) 308–311. doi:10.1038/nature10344.

[38] V.R. Dugyala, M.G. Basavaraj, Control over coffee-ring formation in evaporating liquid drops containing ellipsoids, Langmuir. 30 (2014) 8680–8686. doi:10.1021/la500803h.

[39] V.R. Dugyala, H. Lama, D.K. Satapathy, M.G. Basavaraj, Role of particle shape anisotropy on crack formation in drying of colloidal suspension, Sci. Rep. 6 (2016) 30708. doi:10.1038/srep30708.

[40] X. Zhong, H. Xie, F. Duan, Deposition patterns from evaporating sessile droplets with suspended mixtures of multi-sized and multi-species hydrophilic and non-adsorbing nanoparticles, Appl. Therm. Eng. 111 (2017) 1565–1572. doi:10.1016/j.applthermaleng.2016.08.040.

[41] V.H. Chhasatia, Y. Sun, Interaction of bi-dispersed particles with contact line in an evaporating colloidal drop, Soft Matter. 7 (2011) 10135–10143. doi:10.1039/C1SM06393F.

[42] Y.-F. Li, Y.-J. Sheng, H.-K. Tsao, Evaporation stains: suppressing the coffee-ring effect by contact angle hysteresis, Langmuir. 29 (2013) 7802–7811. doi:10.1021/la400948e.

[43] H. Jeong, J. van Tiem, Y.B. Gianchandani, J. Park, Nano-particle separation using Marangoni flow in evaporating droplets, in: Solid-State Sensors, Actuators Microsystems Work., Hilton Head Island, 2014: pp. 223–226. http://wims2.org/publications/papers/nano-particle_j-park.pdf.

[44] N.D. Patil, P.G. Bange, R. Bhardwaj, A. Sharma, Effects of substrate heating and wettability on evaporation dynamics and deposition patterns for a sessile water droplet containing colloidal particles, Langmuir. 32 (2016) 11958–11972. doi:10.1021/acs.langmuir.6b02769.

[45] H.H. Lee, S.C. Fu, C.Y. Tso, C.Y.H. Chao, Study of residue patterns of aqueous nanofluid droplets with different particle sizes and concentrations on different substrates, Int. J. Heat Mass Transf. 105 (2017) 230–236.

doi:10.1016/j.ijheatmasstransfer.2016.09.093.

[46] X. Zhong, J. Ren, F. Duan, Wettability effect on evaporation dynamics and crystalline patterns of sessile saline droplets, J. Phys. Chem. B. 121 (2017) 7924–7933. doi:10.1021/acs.jpcb.7b03690.

[47] Y. Li, C. Lv, Z. Li, D. Quéré, Q. Zheng, From coffee rings to coffee eyes, Soft Matter. 11 (2015) 4669–4673. doi:10.1039/C5SM00654F.

[48] X. Zhong, F. Duan, Disk to dual ring deposition transformation in evaporating nanofluid droplets from substrate cooling to heating, Phys. Chem. Chem. Phys. 18 (2016) 20664–20671. doi:10.1039/C6CP03231A.

[49] X. Zhong, F. Duan, Flow regime and deposition pattern of evaporating binary mixture droplet suspended with particles, Eur. Phys. J. E. 39 (2016) 18. doi:10.1140/epje/i2016-16018-5.

[50] A. Bar-Cohen, M. Arik, M. Ohadi, Direct liquid cooling of high flux micro and nano electronic components, Proc. IEEE. 94 (2006) 1549–1570. doi:10.1109/JPROC.2006.879791.

[51] X. Zhang, J. Wang, L. Bao, E. Dietrich, R.C.A. van der Veen, S. Peng, J. Friend, H.J.W. Zandvliet, L. Yeo, D. Lohse, Mixed mode of dissolving immersed nanodroplets at a solid–water interface, Soft Matter. 11 (2015) 1889–1900. doi:10.1039/C4SM02397H.

[52] A.K. Panwar, S.K. Barthwal, S. Ray, Effect of evaporation on the contact angle of a sessile drop on solid substrates, J. Adhes. Sci. Technol. 17 (2003) 1321–1329. doi:10.1163/156856103769172760.

[53] K.S. Birdi, D.T. Vu, A. Winter, A study of the evaporation rates of small water drops

placed on a solid surface, J. Phys. Chem. 93 (1989) 3702–3703. doi:10.1021/j100346a065.

[54] H. Hu, R.G. Larson, Evaporation of a sessile droplet on a substrate, J. Phys. Chem. B. 106 (2002) 1334–1344. doi:10.1021/jp0118322.

[55] H.Y. Erbil, G. McHale, M.I. Newton, Drop evaporation on solid surfaces: Constant contact angle mode, Langmuir. 18 (2002) 2636–2641. doi:10.1021/la011470p.

[56] G. McHale, S.M. Rowan, M.I. Newton, M.K. Banerjee, Evaporation and the wetting of a low-energy solid surface, J. Phys. Chem. B. 102 (1998) 1964–1967. doi:10.1021/jp972552i.

[57] R.. Picknett, R. Bexon, The evaporation of sessile or pendant drops in still air, J. Colloid Interface Sci. 61 (1977) 336–350. doi:10.1016/0021-9797(77)90396-4.

[58] M.E.R. Shanahan, Simple theory of "Stick-Slip" wetting hysteresis, Langmuir. 11 (1995) 1041–1043. doi:10.1021/la00003a057.

[59] D. Orejon, K. Sefiane, M.E.R. Shanahan, Stick–Slip of evaporating droplets: Substrate hydrophobicity and nanoparticle concentration, Langmuir. 27 (2011) 12834–12843. doi:10.1021/la2026736.

[60] A. Askounis, Surface nano-patterning using the coffee-stain effect, Univeristy of Edinburgh, 2014.

[61] W. Sempels, R. De Dier, H. Mizuno, J. Hofkens, J. Vermant, Auto-production of biosurfactants reverses the coffee ring effect in a bacterial system, Nat. Commun. 4 (2013) 1757. doi:10.1038/ncomms2746.

[62] H. Hu, R.G. Larson, Analysis of the microfluid flow in an evaporating sessile droplet, Langmuir. 21 (2005) 3963–3971. doi:10.1021/la047528s.

[63] R. Chen, L. Zhang, D. Zang, W. Shen, Wetting and drying of colloidal droplets: Physics and pattern formation, in: M.M. Rahman, A.M. Asiri (Eds.), Adv. Colloid Sci., InTech, 2016: pp. 3–25. doi:10.5772/65301.

[64] H. Hu, R.G. Larson, Analysis of the effects of Marangoni stresses on the microflow in an evaporating sessile droplet., Langmuir. 21 (2005) 3972–3980. doi:10.1021/la0475270.

[65] C.A. Ward, F. Duan, Turbulent transition of thermocapillary flow induced by water evaporation, Phys. Rev. E. 69 (2004) 56308. doi:10.1103/PhysRevE.69.056308.

[66] J.-H. Kim, S.-B. Park, J.H. Kim, W.-C. Zin, Polymer transports inside evaporating water droplets at various substrate temperatures, J. Phys. Chem. C. 115 (2011) 15375–15383. doi:10.1021/jp202429p.

[67] Y. Zhang, Y. Qian, Z. Liu, Z. Li, D. Zang, Surface wrinkling and cracking dynamics in the drying of colloidal droplets, Eur. Phys. J. E. 37 (2014) 84. doi:10.1140/epje/i2014-14084-3.

[68] V. Dugas, J. Broutin, E. Souteyrand, Droplet evaporation study applied to DNA chip manufacturing, Langmuir. 21 (2005) 9130–9136. doi:10.1021/la050764y.

[69] J. Park, J. Moon, Control of colloidal particle deposit patterns within picoliter droplets ejected by ink-jet printing, Langmuir. 22 (2006) 3506–3513. doi:10.1021/la053450j.

[70] H. Hu, R.G. Larson, Marangoni effect reverses coffee-ring depositions, J. Phys. Chem. B. 110 (2006) 7090–7094. doi:10.1021/jp0609232.

[71] M. Majumder, C.S. Rendall, J.A. Eukel, J.Y.L. Wang, N. Behabtu, C.L. Pint, T.-Y. Liu, A.W. Orbaek, F. Mirri, J. Nam, A.R. Barron, R.H. Hauge, H.K. Schmidt, M. Pasquali, Overcoming the "coffee-stain" effect by compositional Marangoni-flow-assisted drop-drying, J. Phys. Chem. B. 116 (2012) 6536–6542. doi:10.1021/jp3009628.

[72] A.K. Thokchom, Q. Zhou, D.-J. Kim, D. Ha, T. Kim, Characterizing self-assembly and deposition behavior of nanoparticles in inkjet-printed evaporating droplets, Sensors Actuators B Chem. 252 (2017) 1063–1070. doi:10.1016/j.snb.2017.06.045.

[73] D.M. Kuncicky, O.D. Velev, Surface-guided templating of particle assemblies inside drying sessile droplets, Langmuir. 24 (2008) 1371–1380. doi:10.1021/la702129b.

[74] J.R. Moffat, K. Sefiane, M.E.R. Shanahan, Effect of TiO2 nanoparticles on contact line stick−slip behavior of volatile drops, J. Phys. Chem. B. 113 (2009) 8860–8866. doi:10.1021/jp902062z.

[75] R. Bhardwaj, X. Fang, P. Somasundaran, D. Attinger, Self-assembly of colloidal particles from evaporating droplets: Role of DLVO interactions and proposition of a phase diagram, Langmuir. 26 (2010) 7833–7842. doi:10.1021/la9047227.

[76] T.P. Bigioni, X.-M. Lin, T.T. Nguyen, E.I. Corwin, T. a Witten, H.M. Jaeger, Kinetically driven self assembly of highly ordered nanoparticle monolayers, Nat. Mater. 5 (2006) 265–270. doi:10.1038/nmat1611.

[77] Y. Li, Q. Yang, M. Li, Y. Song, Rate-dependent interface capture beyond the coffee-ring effect, Sci. Rep. 6 (2016) 24628. doi:10.1038/srep24628.

[78] K. Uno, K. Hayashi, T. Hayashi, K. Ito, H. Kitano, Particle adsorption in evaporating droplets of polymer latex dispersions on hydrophilic and hydrophobic surfaces, Colloid

Polym. Sci. 276 (1998) 810–815. doi:10.1007/s003960050314.

[79] X. Shen, C.-M. Ho, T.-S. Wong, Minimal size of coffee ring structure, J. Phys. Chem. B. 114 (2010) 5269–5274. doi:10.1021/jp912190v.

[80] H. Kim, F. Boulogne, E. Um, I. Jacobi, E. Button, H.A. Stone, Controlled uniform coating from the interplay of Marangoni flows and surface-adsorbed macromolecules, Phys. Rev. Lett. 116 (2016) 124501. doi:10.1103/PhysRevLett.116.124501.

[81] C. Seo, D. Jang, J. Chae, S. Shin, Altering the coffee-ring effect by adding a surfactant-like viscous polymer solution, Sci. Rep. 7 (2017) 500. doi:10.1038/s41598-017-00497-x.

[82] D. Orejon, A study of nanosuspension droplets free evaporation and electrowetting, University of Edinburgh, 2013.

[83] K. Sefiane, On the role of structural disjoining pressure and contact line pinning in critical heat flux enhancement during boiling of nanofluids, Appl. Phys. Lett. 89 (2006) 44106. doi:10.1063/1.2222283.

[84] M. Anyfantakis, D. Baigl, Manipulating the coffee-ring effect: Interactions at work, ChemPhysChem. 16 (2015) 2726–2734. doi:10.1002/cphc.201500410.

[85] J. Wu, J. Xia, W. Lei, B. Wang, Generation of the smallest coffee-ring structures by solute crystallization reaction on a hydrophobic surface, RSC Adv. 3 (2013) 5328. doi:10.1039/c3ra40465j.

[86] J.R. Moffat, K. Sefiane, M.E.R. Shanahan, Nanofluid droplet evaporation kinetics and wetting dynamics on flat substrates, J. Nano Res. 7 (2009) 75–80. doi:10.4028/www.scientific.net/JNanoR.7.75.

[87] E. Adachi, A.S. Dimitrov, K. Nagayama, Stripe patterns formed on a glass surface during droplet evaporation, Langmuir. 11 (1995) 1057–1060. doi:10.1021/la00004a003.

[88] E. Pauliac-Vaujour, P. Moriarty, Meniscus-mediated organization of colloidal nanoparticles, J. Phys. Chem. C. 111 (2007) 16255–16260. doi:10.1021/jp074152t.

[89] E. Pauliac-Vaujour, A. Stannard, C.P. Martin, M.O. Blunt, I. Notingher, P.J. Moriarty, I. Vancea, U. Thiele, Fingering instabilities in dewetting nanofluids, Phys. Rev. Lett. 100 (2008) 176102. doi:10.1103/PhysRevLett.100.176102.

[90] I. Vancea, U. Thiele, E. Pauliac-Vaujour, A. Stannard, C.P. Martin, M.O. Blunt, P.J. Moriarty, Front instabilities in evaporatively dewetting nanofluids, Phys. Rev. E. 78 (2008) 41601. doi:10.1103/PhysRevE.78.041601.

[91] A. Crivoi, F. Duan, Evaporation-induced branched structures from sessile nanofluid droplets, J. Phys. Chem. C. 117 (2013) 7835–7843. doi:10.1021/jp312021w.

[92] R. De Dier, W. Sempels, J. Hofkens, J. Vermant, Thermocapillary fingering in surfactant-laden water droplets, Langmuir. 30 (2014) 13338–13334. doi:10.1021/la503655j.

[93] A.M. Cazabat, F. Heslot, S.M. Troian, P. Carles, Fingering instability of thin spreading films driven by temperature gradients, Nature. 346 (1990) 824–826. doi:10.1038/346824a0.

[94] F. Melo, J.F. Joanny, S. Fauve, Fingering instability of spinning drops, Phys. Rev. Lett. 63 (1989) 1958–1961. doi:10.1103/PhysRevLett.63.1958.

[95] B.D. Edmonstone, O.K. Matar, R.V. Craster, Surfactant-induced fingering phenomena in thin film flow down an inclined plane, Phys. D Nonlinear Phenom. 209 (2005) 62–

79. doi:10.1016/j.physd.2005.06.014.

[96] B.M. Weon, J.H. Je, Fingering inside the coffee ring, Phys. Rev. E. 87 (2013) 13003. doi:10.1103/PhysRevE.87.013003.

[97] L. Pauchard, F. Parisse, C. Allain, Influence of salt content on crack patterns formed through colloidal suspension desiccation, Phys. Rev. E. 59 (1999) 3737–3740. doi:10.1103/PhysRevE.59.3737.

[98] C.C. Annarelli, J. Fornazero, J. Bert, J. Colombani, Crack patterns in drying protein solution drops, Eur. Phys. J. E. 5 (2001) 599–603. doi:10.1007/s101890170043.

[99] D. Mal, S. Sinha, T.R. Middya, S. Tarafdar, Desiccation crack patterns in drying laponite gel formed in an electrostatic field, Appl. Clay Sci. 39 (2008) 106–111. doi:10.1016/j.clay.2007.05.005.

[100] G. Jing, J. Ma, Formation of circular crack pattern in deposition self-assembled by drying nanoparticle suspension, J. Phys. Chem. B. 116 (2012) 6225–6231. doi:10.1021/jp301872r.

[101] B. Sobac, D. Brutin, Desiccation of a sessile drop of blood: Cracks, folds formation and delamination, Colloids Surfaces A Physicochem. Eng. Asp. 448 (2014) 34–44. doi:10.1016/j.colsurfa.2014.01.076.

[102] L. Bahmani, M. Neysari, M. Maleki, The study of drying and pattern formation of whole human blood drops and the effect of thalassaemia and neonatal jaundice on the patterns, Colloids Surfaces A Physicochem. Eng. Asp. 513 (2017) 66–75. doi:10.1016/j.colsurfa.2016.10.065.

[103] Y.Y. Tarasevich, I.V. Vodolazskaya, O.P. Bondarenko, Modeling of spatial–temporal

distribution of the components in the drying sessile droplet of biological fluid, Colloids Surfaces A Physicochem. Eng. Asp. 432 (2013) 99–103. doi:10.1016/j.colsurfa.2013.04.069.

[104] T.A. Yakhno, V.G. Yakhno, A.G. Sanin, O.A. Sanina, A.S. Pelyushenko, N.A. Egorova, I.G. Terentiev, S.V. Smetanina, O.V. Korochkina, E.V. Yashukova, The informative-capacity phenomenon of drying drops, IEEE Eng. Med. Biol. Mag. 24 (2005) 96–104. doi:10.1109/MEMB.2005.1411354.

[105] G. Chen, G. J. Mohamed, Complex protein patterns formation via salt-induced self-assembly and droplet evaporation, Eur. Phys. J. E. 33 (2010) 19–26. doi:10.1140/epje/i2010-10649-4.

[106] D. Kaya, V.A. Belyi, M. Muthukumar, Pattern formation in drying droplets of polyelectrolyte and salt, J. Chem. Phys. 133 (2010) 114905. doi:10.1063/1.3493687.

[107] T.A. Yakhno, V. V. Kazakov, O.A. Sanina, A.G. Sanin, V.G. Yakhno, Drops of biological fluids drying on a hard substrate: Variation of the morphology, weight, temperature, and mechanical properties, Tech. Phys. 55 (2010) 929–935. doi:10.1134/S1063784210070030.

[108] Y.Y. Tarasevich, A.K. Ayupova, Effect of diffusion on the separation of components in a biological fluid upon wedge-shaped dehydration, Tech. Phys. 48 (2003) 535–540. doi:10.1134/1.1576463.

[109] M.E. Buzoverya, Y.P. Shcherbak, I. V. Shishpor, Experimental investigation of the serum albumin fascia microstructure, Tech. Phys. 57 (2012) 1270–1276. doi:10.1134/S1063784212090071.

[110] T.A. Yakhno, Complex pattern formation in sessile droplets of protein-salt solutions with low protein content. What substance fabricates these patterns?, Phys. Chem. 1 (2012) 10–13. doi:10.5923/j.pc.20110101.02.

[111] T.A. Yakhno, Sodium chloride crystallization from drying drops of albumin–salt solutions with different albumin concentrations, Tech. Phys. 60 (2015) 1601–1608. doi:10.1134/S1063784215110262.

[112] A. Crivoi, F. Duan, Fingering structures inside the coffee-ring pattern, Colloids Surfaces A Physicochem. Eng. Asp. 432 (2013) 119–126. doi:10.1016/j.colsurfa.2013.04.051.

[113] T.A.H. Nguyen, M.A. Hampton, A. V Nguyen, Evaporation of nanoparticle droplets on smooth hydrophobic surfaces: The inner coffee ring deposits, J. Phys. Chem. C. 117 (2013) 4707–4716. doi:10.1021/jp3126939.

[114] M.E. Buzoverya, Y.P. Shcherbak, I. V Shishpor, Quantitative estimation of the microstructural inhomogeneity of biological fluid facies, Tech. Phys. 59 (2014) 1550–1555. doi:10.1134/S1063784214100119.

[115] Y. Choi, J. Han, C. Kim, Pattern formation in drying of particle-laden sessile drops of polymer solutions on solid substrates, Korean J. Chem. Eng. 28 (2011) 2130–2136. doi:10.1007/s11814-011-0084-7.

[116] S. Ryu, J.Y. Kim, S.Y. Kim, B.M. Weon, Drying-mediated patterns in colloid-polymer suspensions, Sci. Rep. 7 (2017) 1–7. doi:10.1038/s41598-017-00932-z.

[117] J. Fukai, H. Ishizuka, Y. Sakai, M. Kaneda, M. Morita, A. Takahara, Effects of droplet size and solute concentration on drying process of polymer solution droplets deposited on homogeneous surfaces, Int. J. Heat Mass Transf. 49 (2006) 3561–3567.

doi:10.1016/j.ijheatmasstransfer.2006.02.049.

[118] J.C. Loudet, A.M. Alsayed, J. Zhang, A.G. Yodh, Capillary interactions between anisotropic colloidal particles, Phys. Rev. Lett. 94 (2005) 18301. doi:10.1103/PhysRevLett.94.018301.

[119] J.C. Loudet, A.G. Yodh, B. Pouligny, Wetting and contact lines of micrometer-sized ellipsoids, Phys. Rev. Lett. 97 (2006) 18304. doi:10.1103/PhysRevLett.97.018304.

[120] N. Bowden, F. Arias, T. Deng, G.M. Whitesides, Self-assembly of microscale objects at a liquid/liquid interface through lateral capillary forces, Langmuir. 17 (2001) 1757–1765. doi:10.1021/la001447o.

[121] A.B.D. Brown, C.G. Smith, A.R. Rennie, Fabricating colloidal particles with photolithography and their interactions at an air-water interface, Phys. Rev. E. 62 (2000) 951–960. doi:10.1103/PhysRevE.62.951.

[122] B. Madivala, S. Vandebril, J. Fransaer, J. Vermant, Exploiting particle shape in solid stabilized emulsions, Soft Matter. 5 (2009) 1717. doi:10.1039/b816680c.

[123] B. Madivala, J. Fransaer, J. Vermant, Self-assembly and rheology of ellipsoidal particles at interfaces, Langmuir. 25 (2009) 2718–2728. doi:10.1021/la803554u.

[124] B.J. Park, E.M. Furst, Attractive interactions between colloids at the oil–water interface, Soft Matter. 7 (2011) 7676. doi:10.1039/c1sm00005e.

[125] J.-B. Fournier, P. Galatola, Anisotropic capillary interactions and jamming of colloidal particles trapped at a liquid-fluid interface, Phys. Rev. E. 65 (2002) 31601. doi:10.1103/PhysRevE.65.031601.

[126] A.P. Sommer, M. Ben-Moshe, S. Magdassi, Size-discriminative self-assembly of nanospheres in evaporating drops, J. Phys. Chem. B. 108 (2004) 8–10. doi:10.1021/jp0363747.

[127] J.-Y. Jung, Y.W. Kim, J.Y. Yoo, Behavior of particles in an evaporating didisperse colloid droplet on a hydrophilic surface, Anal. Chem. 81 (2009) 8256–8259. doi:10.1021/ac901247c.

[128] T.S. Wong, T.H. Chen, X. Shen, C.M. Ho, Nanochromatography driven by the coffee ring effect, Anal. Chem. 83 (2011) 1871–1873. doi:10.1021/ac102963x.

[129] V.H. Chhasatia, A.S. Joshi, Y. Sun, Effect of relative humidity on contact angle and particle deposition morphology of an evaporating colloidal drop, Appl. Phys. Lett. 97 (2010) 231909. doi:10.1063/1.3525167.

[130] Y.-C. Hu, Q. Zhou, H.-M. Ye, Y.-F. Wang, L.-S. Cui, Peculiar surface profile of poly(ethylene oxide) film with ring-like nucleation distribution induced by Marangoni flow effect, Colloids Surfaces A Physicochem. Eng. Asp. 428 (2013) 39–46. doi:10.1016/j.colsurfa.2013.03.035.

[131] E. Hendarto, Y.B. Gianchandani, Size sorting of floating spheres based on Marangoni forces in evaporating droplets, J. Micromechanics Microengineering. 23 (2013) 75016. doi:10.1088/0960-1317/23/7/075016.

[132] X. Zhong, C. Wu, F. Duan, From enhancement to elimination of dual-ring pattern of nanoparticles from sessile droplets by heating the substrate, Appl. Therm. Eng. 115 (2017) 1418–1423. doi:10.1016/j.applthermaleng.2016.11.002.

[133] M. Parsa, S. Harmand, K. Sefiane, M. Bigerelle, R. Deltombe, Effect of substrate

temperature on pattern formation of bidispersed particles from volatile drops, J. Phys. Chem. B. 121 (2017) 11002–11017. doi:10.1021/acs.jpcb.7b09700.

[134] A. Crivoi, F. Duan, Effect of surfactant on the drying patterns of graphite nanofluid droplets, J. Phys. Chem. B. 117 (2013) 5932–5938. doi:10.1021/jp401751z.

[135] E.L. Talbot, A. Berson, P.S. Brown, C.D. Bain, Drying and deposition of picolitre droplets of colloidal suspensions in binary solvent mixtures, in: NIP28 28th Int. Conf. Digit. Print. Technol. Digit. Fabr., Society for Imaging Science and Technology: Springfield, Quebec, 2012: pp. 420–423. http://www.dspace.cam.ac.uk/handle/1810/243374.

[136] A. Crivoi, F. Duan, Amplifying and attenuating the coffee-ring effect in drying sessile nanofluid droplets, Phys. Rev. E. 87 (2013) 42303. doi:10.1103/PhysRevE.87.042303.

[137] H.B. Eral, D.M. Augustine, M.H.G. Duits, F. Mugele, Suppressing the coffee stain effect: how to control colloidal self-assembly in evaporating drops using electrowetting, Soft Matter. 7 (2011) 4954. doi:10.1039/c1sm05183k.

[138] D. Orejon, K. Sefiane, M.E.R. Shanahan, Evaporation of nanofluid droplets with applied DC potential, J. Colloid Interface Sci. 407 (2013) 29–38. doi:10.1016/j.jcis.2013.05.079.